Abundance ties: Nephele and the globular cluster population accreted with ω Cen

G. Pagnini, P. Di Matteo, M. Haywood, A. Mastrobuono-Battisti, F. Renaud, M. Mondelin, O. Agertz, P. Bianchini, L. Casamiquela, S. Khoperskov, et al.

A&A, 693, A155 (2025)
https://doi.org/10.1051/0004-6361/202450264

Astronomy & Astrophysics

Abundance ties: Nephele and the globular cluster population accreted with ω Cen

Based on APOGEE DR17 and *Gaia* EDR3

G. Pagnini[1,⋆], P. Di Matteo[1], M. Haywood[1], A. Mastrobuono-Battisti[1,2], F. Renaud[3,7], M. Mondelin[4], O. Agertz[5], P. Bianchini[3], L. Casamiquela[1], S. Khoperskov[6], and N. Ryde[5]

[1] GEPI, Observatoire de Paris, PSL Research University, CNRS, Place Jules Janssen, 92195 Meudon, France
[2] Dipartimento di Fisica e Astronomia "Galileo Galilei", Università di Padova, Vicolo dell'Osservatorio 3, 35122 Padova, Italy
[3] Université de Strasbourg, CNRS, Observatoire Astronomique de Strasbourg, 67000 Strasbourg, France
[4] CEA, AIM, Université Paris-Saclay, 91191 Gif-sur-Yvette, France
[5] Division of Astrophysics, Department of Physics, Lund University, Box 118, 221 00 Lund, Sweden
[6] Leibniz Institut für Astrophysik Potsdam (AIP), An der Sternwarte 16, 14482 Potsdam, Germany
[7] University of Strasbourg Institute for Advanced Study, 5 allée du Général Rouvillois, 67083 Strasbourg, France

Received 5 April 2024 / Accepted 20 October 2024

ABSTRACT

Context. The peculiar Galactic globular cluster ω Centauri (NGC 5139) has drawn attention for its unique features, such as an unusually high stellar mass compared to other Galactic globular clusters and a broad distribution of chemical elements. These features have led to the hypothesis that ω Centauri might be the nuclear remnant of an ancient dwarf galaxy accreted by the Milky Way, potentially bringing along its own globular cluster system.
Aims. In this work, we adopt an innovative approach by examining the individual chemical abundances of Galactic globular clusters to identify shared patterns with ω Centauri.
Methods. Applying Gaussian mixture models to globular cluster stars, whose membership is based on the analysis of the *Gaia* EDR3 release, and whose chemical abundances have been obtained from APOGEE DR17, we depart from traditional kinematic-based procedures and search for globular clusters that are chemically compatible with ω Centauri in an eight-dimensional space defined by [Fe/H], α-elements such as [Mg/Fe], [Si/Fe], and [Ca/Fe], light+odd-Z elements such as [C/Fe], [Al/Fe], and [K/Fe], and an iron-peak element as [Mn/Fe]. With this approach, clusters that are chemically compatible with ω Centauri are clusters whose chemical patterns are contained in the abundance domain defined by ω Centauri stars.
Results. Our analysis leads to the identification of six globular clusters – NGC 6752, NGC 6656, NGC 6809, NGC 6273, NGC 6205, and NGC 6254 – that exhibit strong chemical similarities with ω Centauri, and that have metallicities that coincide with those of the two known peaks (primary and secondary) of ω Centauri's metallicity distribution. They all exhibit non-null intrinsic [Fe/H] dispersions, ranging between 0.07 and 0.12 dex, unless the ASPCAP uncertainties had been severely underestimated, and three of them have statistically significant skewed [Fe/H] distributions. Furthermore, the chemical patterns of these clusters lead to the exclusion that they were formed in progenitor galaxies with chemical enrichment histories similar to those of the Large and Small Magellanic Clouds, Sagittarius, and Fornax. Once placed in kinematic spaces such as the energy – angular momentum plane, these clusters result scatter across an extended region, which is predicted by *N*-body simulations if their common progenitor was sufficiently massive compared to the Milky Way.
Conclusions. Our novel approach suggests a common origin for NGC 6752, NGC 6656, NGC 6809, NGC 6273, NGC 6205, NGC 6254, and ω Centauri, indicating that Nephele, as we propose to call the progenitor in which all these clusters formed, played a substantial role in the Galaxy's history. The finding that a set of globular clusters can be associated with ω Centauri reinforces the hypothesis that this system is the remnant of a galaxy, and not simply an unusual globular cluster. This study also shows that the spectroscopic data at our disposal have reached the quality needed to compare chemical patterns of stellar systems, to reveal their common origins or exclude their association with specific progenitor galaxies.

Key words. Galaxy: abundances – Galaxy: formation – globular clusters: general – Galaxy: kinematics and dynamics – globular clusters: individual: omega Centauri (NGC 5139)

1. Introduction

The Galactic globular cluster (GC) ω Centauri (NGC 5139) has been known to be peculiar in many aspects for several decades. Its total stellar mass, estimated to be $3.5 \pm 0.03 \times 10^6\,M_\odot$ (Baumgardt & Hilker 2018), is ten times greater than the mean stellar mass of all known Galactic GCs. Since the early work of Sistero & Fourcade (1970), it has been known that this cluster has a flattened shape, which is accompanied by a significant amount of rotation (Meylan & Mayor 1986; Merritt et al. 1997; Norris et al. 1997; Pancino et al. 2007; Bianchini et al. 2013; Kamann et al. 2018; Sanna et al. 2020) and also a counter-rotating core (Pechetti et al. 2024). It contains stars with an extended [Fe/H] distribution (Norris & Da Costa 1995; Suntzeff & Kraft 1996; Smith et al. 2000; Sollima et al. 2005;

⋆ Corresponding author; giulia.pagnini@obspm.fr

Villanova et al. 2007; Calamida et al. 2009; Johnson & Pilachowski 2010; Pancino et al. 2011; Marino et al. 2011; Nitschai et al. 2023) with values ranging from about −2.2 to −0.4 dex (Mészáros et al. 2021). Not only [Fe/H], but all chemical abundance elements studied so far indicate that ω Cen had a complex formation (among others, see Norris & Da Costa 1995; Hilker et al. 2004; Johnson & Pilachowski 2010; D'Orazi et al. 2011), which is possibly also reflected in its stars having an extended age range (Villanova et al. 2007, 2014). Because of these peculiar properties, it was already suggested more than 20 years ago (Lee et al. 1999; Majewski et al. 2000; Carraro & Lia 2000; Bekki & Freeman 2003; Tsuchiya et al. 2003, 2004) that ω Cen could be the remnant of an ancient dwarf galaxy accreted by the Milky Way (MW) during the first billion years after its formation. In this scenario, the current cluster would be the stellar nucleus of the dwarf, whose stellar envelope would have been stripped during the accretion process, due to the tidal effects exerted by the Galactic potential. The stellar nucleus, much more compact and dense, would have survived the accretion, and continued orbiting the MW since then. Bekki & Freeman (2003) showed that this scenario may explain some of the properties of ω Cen (namely, its current mass and its orbital characteristics) if the host galaxy had an initial stellar mass of about 10^8 $M_\odot$, the nucleus an initial mass of about 6×10^6 $M_\odot$, and a total-to-baryonic mass ratio of 10. Since then, the remnant galaxy and its nucleus would have continued to lose stars (and dark matter) and keep sinking in the inner Galaxy, due to the combined effect of the tidal forces and dynamical friction exerted by the MW. If such a merger occurred in the first few billion years of the formation of our Galaxy, the estimated mass of the ω Cen progenitor is sufficiently large (at least a factor of 1/100 with respect to the mass of the MW, depending on the time of the accretion, see Snaith et al. 2014) to consider it a significant accretion event in the early evolution of our Galaxy.

Given the numbers above, such an accretion event would have contributed to increasing the stellar mass budget of the Galaxy by an amount similar to that of the stellar halo (in this respect, it is interesting to recall the recent discovery of the Fimbulthul stream, which is unequivocally showing that ω Cen is still losing part of its stars in the field, see Ibata et al. 2019), as this dwarf galaxy should have also brought its own GC system to the MW. Galaxies in the local Universe with stellar masses of the order of 10^8 $M_\odot$ can contain up to dozen clusters (Eadie et al. 2022); simulations-based estimates (Kruijssen et al. 2020) of the number of GCs accreted by the MW over time also reinforce that a dozen clusters is a realistic number for a dwarf whose stellar mass was about a hundredth of that of the MW at the time of the accretion. This leads to the questions of where the GCs that the ω Cen progenitor brought with it are, how they are redistributed in the Galaxy, how many there are, and, first of all, how they can be distinguished among all the GCs populating our Galaxy today.

One may be tempted to retrieve the population of GCs lost by the ω Cen progenitor galaxy by simply looking for the population of GCs that today share similar kinematic properties to those of this cluster. Following this approach, for example, Myeong et al. (2019) suggest that ω Cen may be associated with the Sequoia accretion event, while Massari et al. (2019) are more in favour of an association with the *Gaia* Sausage Enceladus galaxy, of which ω Cen would have been the nuclear star cluster (NSC). In both cases, the similarity of the cluster's orbital properties with Sequoia (or *Gaia* Sausage Enceladus) is a decisive argument. An association of ω Cen with Sequoia would mean that this cluster shares a common origin with NGC 5466, IC 4499, NGC 7006, Pal 13, and FSR 1758 (these are indeed the clusters for which the association with Sequoia appears robust, according to Massari et al. 2019), while an association with *Gaia* Sausage Enceladus implies that ω Cen would be associated instead with the GCs NGC 288, NGC 362, NGC 1261, NGC 1851, NGC 1904, NGC 2298, NGC 2808, NGC 4147, NGC 4833, NGC 5286, NGC 5897, NGC 6205, NGC 6229, NGC 6235, NGC 6284, NGC 6341, IC 1257, Djorg 1, Terzan 10, ESO-SC06, NGC 6779, NGC 6864, NGC 7089, NGC 7099, and NGC 7492 (still following Massari et al. 2019, for the list of clusters robustly associated with *Gaia* Sausage Enceladus). These two classifications are thus in conflict, unless Sequoia and *Gaia* Sausage Enceladus are not part of the same progenitor galaxy (Koppelman et al. 2020; Amarante et al. 2022).

In these recent years, however, a number of studies have shown that the association of a group of GCs, as well as of field stars, with a common progenitor on the basis of orbital criteria (namely, their kinematic coherence – the approach followed in the above-cited papers) is not straightforward at all, and even worse, it is not completely physically motivated, unless very specific assumptions are made about the accretion history of our Galaxy (see Jean-Baptiste et al. 2017; Khoperskov et al. 2023b,a). The simulations by Bekki & Freeman (2003) also show that the progenitor galaxy of ω Cen possibly left an extended trail of stars distributed over a wide range of orbital parameters (see Fig. 5 in their article). In Pagnini et al. (2023), we made use of N-body simulations to show that kinematic spaces are not a reliable tool for distinguishing GCs that originate from a single accreted galaxy from the rest of the GC population. In fact, clusters that have different orbital features today may originate from the same progenitor galaxy, just as clusters with similar kinematic properties may actually have a different origin (see Pagnini et al. 2023).

For all these reasons, in this work we have chosen to investigate the population of GCs associated with the progenitor of ω Cen by searching for all Galactic GCs that have chemical abundances compatible with those of ω Cen, in a sort of 'chemical tagging' approach (Freeman & Bland-Hawthorn 2002), whereby we look for common chemical patterns between Galactic GCs and ω Cen, based on individual star abundances. Indeed, unlike the orbital characteristics of GCs, which are generally not conserved during an accretion, their chemical properties are linked to those of the interstellar medium (hereafter ISM) in which these clusters were formed. We have therefore taken a new approach compared to those proposed so far in the literature, and taken advantage of the wealth of new spectroscopic homogeneous data available for tens of Galactic GCs, to search for their common characteristics in abundance spaces. For this, we searched for all GCs in the recently published catalogue of Schiavon et al. (2024), based on APOGEE DR17 data (Abdurro'uf et al. 2022), that are chemically compatible with ω Cen; that is, whose distribution in chemical abundance spaces is contained within that of ω Cen. Indeed, if ω Cen were the nucleus of a dwarf galaxy, its chemical abundance patterns should be representative (at least of part) of the chemical abundance patterns of its progenitor (as we shall show to be the case for the M54-Sagittarius dwarf system in Appendix C, available on Zenodo), which in turn reflect those of the ISM in which the progenitor stellar populations formed, at a given time. In other words, the chemical abundances of GCs, as well as of field stars, formed in the ω Cen progenitor should be representative of the chemical enrichment history of the progenitor galaxy itself; that is, they should trace specific epochs of this evolution. We can use the NSC of this progenitor galaxy – that is, ω Cen itself – as representative of at least part of the progenitor chemical evolution,

based on the chemical similarities that exist, as we shall show, between the Sagittarius dwarf galaxy and M54, its NSC.

Our analysis allows us to identify six GCs – namely, NGC 6752, NGC 6656, NGC 6809, NGC 6273, NGC 6205, and NGC 6254 – that have chemical patterns found also in ω Cen, and that also show some common characteristics in their metallicity distribution function (MDF) – all results that we interpret as evidence of their common origin. NGC 5024, NGC 6544, FSR 1758, and NGC 1904 may also be part of this same group, but – as we shall see – the analysis of these clusters is based on statistics that are too weak to allow us to derive any firm conclusions. According to the analysis presented in this paper, Nephele[1], as we propose to call the progenitor of ω Centauri, in which all these clusters formed, has potentially brought at least six clusters to the MW, proving to be a significant accretion in the history of our Galaxy.

The paper is organised as follows. We describe in Sect. 2 the observational dataset used for this study, and in Sect. 3 the method used to analyse it. In Sect. 4, we present the obtained results. Finally, after a discussion in Sect. 5, in Sect. 6, we derive our conclusions.

2. Observational data

For this study, we have made use of data from the APOGEE Value Added Catalogue (VAC) of Galactic GC stars (see Schiavon et al. 2024). The catalogue comprises a total of 7737 entries for 6422 unique stars associated with 72 Galactic GCs and contains full APOGEE DR17 information (Abdurro'uf et al. 2022) including radial velocities and abundances for up to 20 elements[2]. As in Horta et al. (2023), among these stars, only those satisfying the following criteria have been used for this study:

1. a signal-to-noise ratio of `SNREV` > `70`;
2. temperatures in the range of 3500 K < T_{eff} < 5500 K and surface gravities of log g < 3.6;
3. `APOGEE STARFLAG and APOGEE STARBAD` = `0`;
4. stars that have, according to Vasiliev & Baumgardt (2021), a high probability of being members of the cluster (`VB_PROB` ≥ 0.9).

With these selections, the number of GC stars reduces from 6422 (before selection) to 3223 (after selection), corresponding to 57 Galactic GCs.

3. Methods

To assess whether a given GC is compatible, in the chemical abundance space, with ω Cen, we made use of a Gaussian mixture model (GMM) approach. We considered a high-precision eight-dimensional abundance space defined by [Fe/H], the α elements [Mg/Fe], [Si/Fe], and [Ca/Fe], the light+odd-Z elements [C/Fe], [Al/Fe], and [K/Fe], and the iron-peak element [Mn/Fe][3], and we kept only the stars in the Schiavon et al. (2024) catalogue for which all the abundance flags of these elements are equal to zero. In this way, we covered several nucleosynthetic channels. The different α-elements have slightly different origins and Mg is the best determined APOGEE-element. Al and Mg are anti-correlated in GCs at low metallicities (Pancino et al. 2017), and carbon, although its abundance changes due to internal processes within red giant stars, could be further evidence in favour of a common origin. With this choice, the number of stars used for the GMM analysis described below reduces to 2077, associated with 54 different GCs. For all the elements listed above, the median uncertainty is smaller than 0.07. We note that the choice to use eight elements for the GMM analysis is a compromise between two different needs. On the one hand, the higher the number of abundances used, the higher the probability of identifying clusters that are chemically similar to ω Cen (two clusters may have similar abundances of some elements, but not in others, so using enough abundances allows us to better discriminate clusters from each other; for a discussion on this point, see Sect. 4.3). On the other hand, the higher the number of elements used, the lower the number of stars per cluster (the flags imposed on the quality of each chemical abundance imply that the number of stars meeting the quality criteria on all abundances decreases as the number of elements used increases). We therefore chose to use eight elements as a compromise, but still tested the algorithm with up to 12 elements (namely, [Fe/H], [C/Fe], [N/Fe], [O/Fe], [Al/Fe], [Mg/Fe], [Si/Fe], [Ca/Fe], [K/Fe], [Mn/Fe], and [Ni/Fe]) and found that the results presented in the following of this paper were consistent. In particular, as we shall show in Appendix D (available on Zenodo), the chemical compatibility between ω Cen and the clusters found using this approach extends also to chemical elements not used for the GMM analysis, [Na/Fe] and [Ce/Fe], for which the corresponding uncertainties are large (≃0.17 and ≃0.07), but which are available in the Schiavon et al. (2024) catalogue.

The distribution of ω Cen in the eight-dimensional abundance space defined by [Fe/H], [Mg/Fe], [Si/Fe], [Ca/Fe], [C/Fe], [Al/Fe], [K/Fe], and [Mn/Fe] was then fitted by using an increasing number of Gaussian components and the optimal number of components for our dataset was then determined by minimising the Bayesian information criterion (BIC). With this procedure, we found that the number of components that best reproduces the eight-dimensional distribution of ω Cen is five (see Fig. 1 for their distribution in the [Mg/Fe]-[Fe/H] plane, where outliers of this distribution are also reported, these latter being stars with a probability density below a threshold defined in Sect. 4). As we checked, the number of Gaussian components tends to decrease with the number of chemical elements used in the GMM and we advise the reader against giving a physical meaning to this specific number. Depending on the chemical abundances under study, as well as on the cluster algorithm used, this number may also vary. For example, Johnson & Pilachowski (2010) found that the MDF of ω Cen could be fitted by four components. Mészáros et al. (2021), on the other hand, considered a three-dimensional chemical space (including the [Fe/H], [Al/Fe], and [Mg/Fe] abundances), and found seven groups. The

[1] In Greek mythology, Nephele is the mother of centaurs. We are aware that adding a new name to an already rich list of possible galaxies accreted by the MW over time may be confusing at first sight, but we believe it is important to assign a name to the set of clusters (and, in a future work, of field stars) associated with ω Cen on the basis of the individual abundances of stars, and thus make clear that this association is based on different criteria from the kinematically based ones usually adopted in the literature.

[2] The APOGEE project is based on H-band spectra with resolution of $R \sim 22\,500$ and derives elemental abundances for up to 20 species at a precision of 0.1 dex.

[3] Note that the abundances of elements like K or Mn are based on a few weak lines. Towards the low metallicity end ([Fe/H] < −1.5), ASPCAP may be delivering upper limits only, depending on the star's T_{eff} and log g.

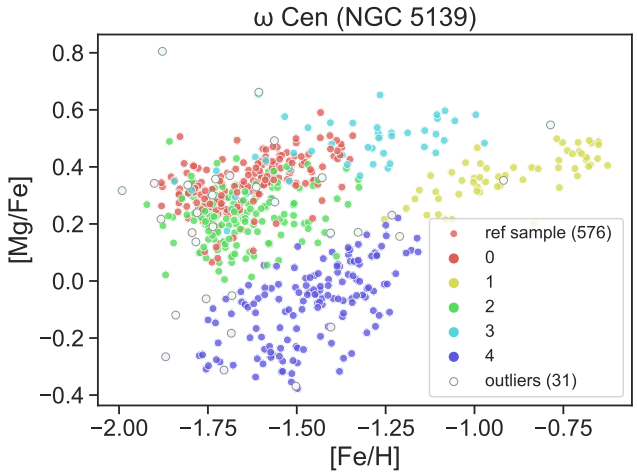

Fig. 1. [Mg/Fe] vs. [Fe/H] distribution of stars belonging to ω Cen, colour-coded according to the different components retrieved when minimising the BIC criterion in the GMM. Filled symbols represent the reference sample of stars of ω Cen (i.e. stars with a probability density above a threshold defined in Sect. 4), while empty symbols are the outliers (i.e. stars below this threshold).

difference in the retrieved number of components may also be due to the different algorithm used to perform the clustering analysis. In particular, the *k-means* algorithm used in Mészáros et al. (2021) relies on centroid-based clustering, which performs particularly well in identifying clusters in a set of data points with a spherical-like structure, while it may perform less well in representing more complex patterns, such as those describing chemical abundances.

For each of the 54 GCs included in this study, we then estimated the fraction of stars that have a high probability of belonging to the GMM model obtained for ω Cen; that is, the fraction of stars whose distribution in the eight-dimensional abundance space falls within that of ω Cen. To estimate the uncertainties on the derived fractions, we repeated this procedure a hundred times, each time bootstrapping the data of both ω Cen and each GC: for each bootstrap realisation, we also took into account the individual uncertainties of the chemical abundances in the Schiavon et al. (2024) catalogue using a Monte-Carlo sampling. As an estimator of the compatibility of each GC in the sample with ω Cen, we used the fraction of compatible stars – that is, the fraction of stars that fall within the distribution of ω Cen in the eight-dimensional chemical spaces according to the GMM – out of the total number of stars in the GC. Compatible stars are defined as those whose log-likelihood exceeds or is equal to a threshold, which we established as the fifth percentile of the log-likelihood distribution of the training dataset; namely, ω Cen. In contrast, outliers are stars with a probability density below the established threshold. The sample of ω Cen stars with a log-likelihood above the fifth percentile threshold is referred to as the 'reference sample'.

4. Results

For each cluster, the fraction of stars that are chemically compatible with ω Cen (in the eight-dimensional space defined in the previous section) out of the total is shown in Table 1 with the corresponding uncertainty obtained by averaging over the fractions derived from the 100 GMM repetitions and computing the standard deviation. The total number of stars in each GC after the selections made (see Sect. 2) is also listed, together with the median and mode of its [Fe/H] distribution. In this table, clusters are ranked according to the fraction of compatible stars, from clusters with the highest level of compatibility to clusters with the lowest. We have proven that this ranking is robust even when changing the threshold or the number of elements considered in the GMM. Apart from the two first GCs reported in Table 1

Table 1. Fraction of stars chemically compatible with ω Cen.

GC name	Fraction (%)	# stars	$[Fe/H]_{median}$	$[Fe/H]_{mode}$
Ter10	98 ± 14	1	−1.62 ± 0.02	−1.60 ± 0.05
NGC 2298	94 ± 22	2	−1.83 ± 0.02	−1.83 ± 0.05
NGC 5139	**89 ± 3**	**607**	**−1.57 ± 0.01**	**−1.66 ± 0.04**
NGC 6752	**84 ± 8**	**83**	**−1.47 ± 0.01**	**−1.47 ± 0.02**
NGC 6656	**81 ± 8**	**68**	**−1.66 ± 0.02**	**−1.64 ± 0.05**
NGC 6809	**79 ± 13**	**18**	**−1.73 ± 0.02**	**−1.73 ± 0.05**
NGC 6273	**76 ± 9**	**40**	**−1.67 ± 0.02**	**−1.69 ± 0.07**
NGC 6205	**69 ± 14**	**26**	**−1.48 ± 0.02**	**−1.48 ± 0.04**
NGC 5024	64 ± 23	5	−1.80 ± 0.02	−1.80 ± 0.03
NGC 6254	**64 ± 15**	**50**	**−1.49 ± 0.01**	**−1.49 ± 0.03**
NGC 6544	56 ± 20	15	−1.47 ± 0.02	−1.48 ± 0.05
FSR1758	56 ± 26	7	−1.40 ± 0.05	−1.41 ± 0.07
NGC 1904	52 ± 18	26	−1.51 ± 0.03	−1.53 ± 0.07
NGC 6093	47 ± 50	1	−1.61 ± 0.01	−1.59 ± 0.04
NGC 7089	44 ± 23	15	−1.48 ± 0.02	−1.48 ± 0.05
NGC 6218	33 ± 19	40	−1.26 ± 0.01	−1.26 ± 0.02
NGC0288	31 ± 22	37	−1.27 ± 0.01	−1.26 ± 0.03
NGC 6380	31 ± 28	9	−0.75 ± 0.03	−0.76 ± 0.05
Ter4	30 ± 46	1	−1.45 ± 0.02	−1.40 ± 0.02
NGC 6121	29 ± 25	169	−1.05 ± 0.00	−1.04 ± 0.01
Djorg_2	24 ± 36	4	−1.07 ± 0.02	−1.07 ± 0.03
NGC 6171	24 ± 21	23	−0.97 ± 0.03	−0.97 ± 0.05
NGC0104	20 ± 19	224	−0.75 ± 0.00	−0.74 ± 0.01
NGC 6522	20 ± 34	2	−1.15 ± 0.07	−1.16 ± 0.10
NGC 6715	16 ± 10	26	−1.41 ± 0.05	−1.52 ± 0.06
HP1	15 ± 20	10	−1.16 ± 0.05	−1.17 ± 0.08
NGC 6838	14 ± 15	45	−0.76 ± 0.01	−0.77 ± 0.04
NGC 6397	13 ± 15	10	−2.01 ± 0.02	−2.02 ± 0.03
NGC 5272	11 ± 7	71	−1.38 ± 0.01	−1.37 ± 0.04
NGC 6723	11 ± 18	7	−1.04 ± 0.02	−1.06 ± 0.05
NGC 6558	11 ± 25	3	−1.15 ± 0.05	−1.15 ± 0.05
NGC 6569	11 ± 19	6	−0.99 ± 0.02	−1.00 ± 0.03
Ter9	10 ± 15	9	−1.39 ± 0.04	−1.40 ± 0.06
NGC 3201	8 ± 8	98	−1.35 ± 0.01	−1.34 ± 0.02
NGC 6642	8 ± 21	6	−1.03 ± 0.29	−1.04 ± 0.23
Ter2	5 ± 17	2	−0.84 ± 0.04	−0.86 ± 0.06
NGC 5904	3 ± 5	79	−1.20 ± 0.01	−1.20 ± 0.04
NGC 6316	2 ± 10	6	−0.76 ± 0.02	−0.77 ± 0.03
NGC 6717	2 ± 14	2	−1.17 ± 0.04	−1.16 ± 0.06
NGC 6760	1 ± 10	3	−0.73 ± 0.02	−0.73 ± 0.03
NGC 6229	1 ± 7	3	−1.27 ± 0.02	−1.27 ± 0.03
NGC 1851	1 ± 3	31	−1.12 ± 0.02	−1.14 ± 0.02
NGC 7078	0 ± 0	1	−2.24 ± 0.01	−2.19 ± 0.01
Ter5	0 ± 0	2	−0.61 ± 0.01	−0.59 ± 0.03
Pal6	0 ± 0	1	−0.92 ± 0.01	−0.89 ± 0.05
NGC 6341	0 ± 0	3	−2.20 ± 0.04	−2.19 ± 0.04
NGC 6553	0 ± 0	1	−0.22 ± 0.01	−0.20 ± 0.05
NGC 6388	0 ± 0	24	−0.51 ± 0.02	−0.53 ± 0.05
NGC 6304	0 ± 0	5	−0.49 ± 0.05	−0.51 ± 0.06
NGC 6293	0 ± 0	1	−2.08 ± 0.02	−2.03 ± 0.02
NGC 4590	0 ± 0	1	−2.12 ± 0.01	−2.07 ± 0.01
NGC 2808	0 ± 0	98	−1.09 ± 0.01	−1.10 ± 0.02
NGC0362	0 ± 1	48	−1.11 ± 0.01	−1.11 ± 0.01
Ton2	0 ± 5	2	−0.61 ± 0.01	−0.61 ± 0.04

Notes. Clusters for which this fraction is higher than 60%, and which – after the selections described in Sects. 2 and 3 – contain at least 15 stars, are marked in bold. For each cluster, the number of stars used for the analysis, the median, and the mode of [Fe/H] distribution are reported.

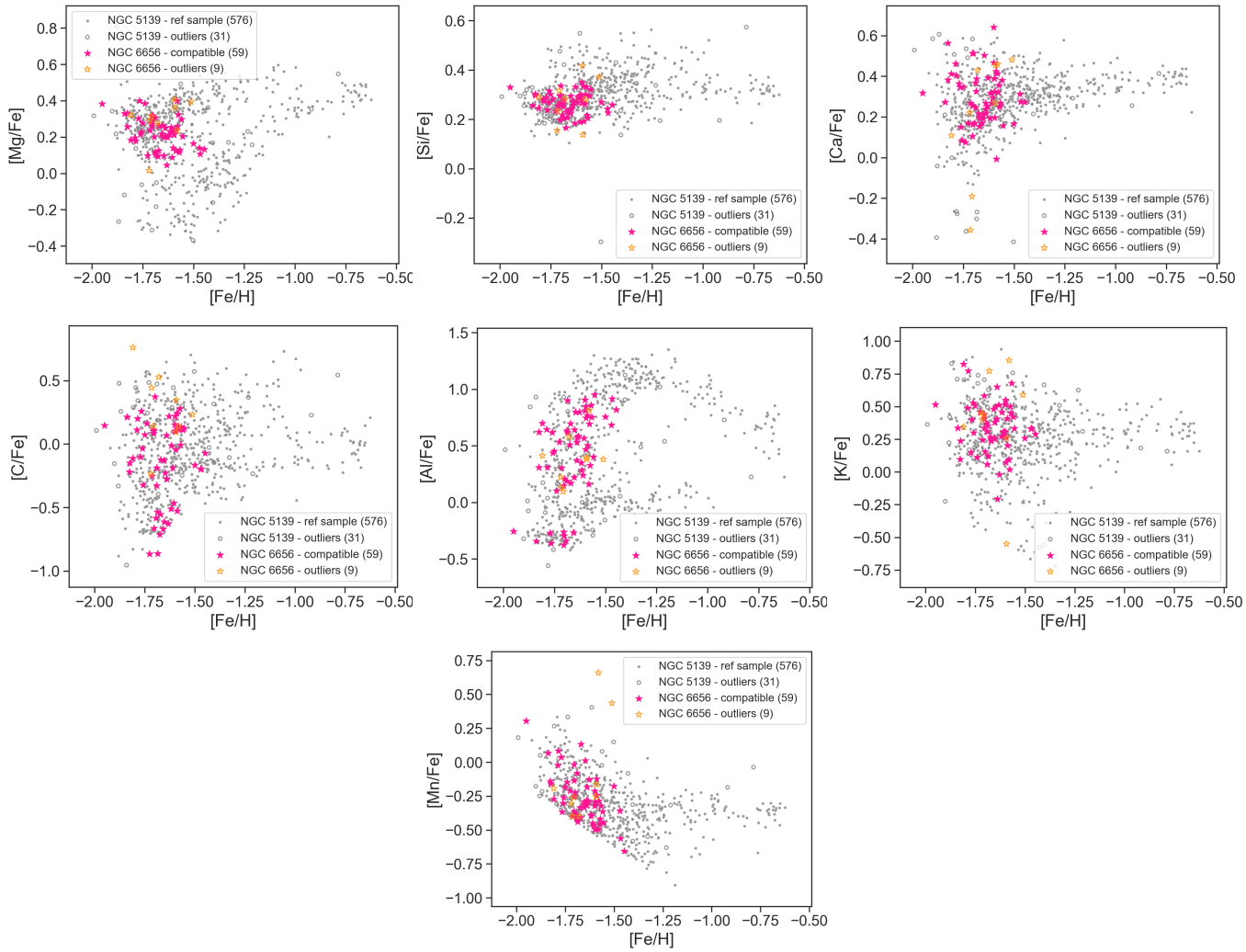

Fig. 2. Chemical abundance relations for members of NGC 6656 (colour) and ω Cen (grey). The filled symbols show the reference sample of ω Cen (grey) and the stars of NGC 6656 (magenta) chemically compatible with it according to the GMM (see Sect. 4), while the empty ones (grey and orange colours) correspond to their outliers. The number of stars in each category is reported in parentheses.

(Ter 10 and NGC 2298), for which the large fraction of stars overlapping with ω Cen is based on the analysis of only one and two stars, respectively, a result that we do not consider meaningful given the low statistics on which it is based, the third most compatible GC in the analysis is ω Cen itself. This result appears trivial, and indeed it is, but we checked this compatibility firstly to test that the whole procedure is correct and secondly to establish the compatibility fraction of two distributions (the training ω Cen eight-dimensional dataset and the 'GC=ω Cen' eight-dimensional dataset) drawn from the same initial set of stars through the bootstrap process described in the previous section. With a threshold for outliers detection fixed at the fifth percentile of the log-likelihood distribution of the ω Cen GMM model, we see that the fraction of the reference sample of stars in ω Cen, averaged over 100 bootstraps, is 89%. This compatibility fraction essentially sets the upper limit that we can expect to find for all other clusters, compared to ω Cen.

4.1. [X/Fe] versus [Fe/H] planes for globular clusters chemically compatible with ω Cen

Apart from ω Cen itself, the GMM finds four GCs (with a total number of stars greater than 15) that have a fraction of stars compatible with ω Cen that is greater than 70%; namely, NGC 6752, NGC 6809 (M 55), NGC 6273 (M 19), and NGC 6656 (M 22). Three additional clusters – namely, NGC 6254 (M 10), NGC 5024, and NGC 6205 (M 13) – have a fraction of stars chemically compatible with ω Cen between 60 and 70%; however, the limited number of stars (5) available for NGC 5024 prevents us from drawing strong conclusions about this cluster. In Figs. 2 and 3 (and Figures in Appendix A, available on Zenodo), we report the distributions in [X/Fe] versus [Fe/H] spaces for all these clusters (except for NGC 5024 for the reason given above), and for all [X/Fe] abundances used to build the ω Cen GMM model. We emphasise that while these figures report two-dimensional projections of abundance spaces, the GMM model has been built by making use of the whole eight-dimensional abundance space, and not by estimating the chemical compatibility for each of these projections separately. In all panels of these figures, the corresponding distribution of ω Cen stars is also reported for comparison. For all clusters in these figures, compatible stars and outliers are shown with different colours or symbols, to visually show the result of the GMM classification.

Examination of Figs. 2 and 3 (together with the figures in Appendix A on Zenodo) reveals some interesting characteristics

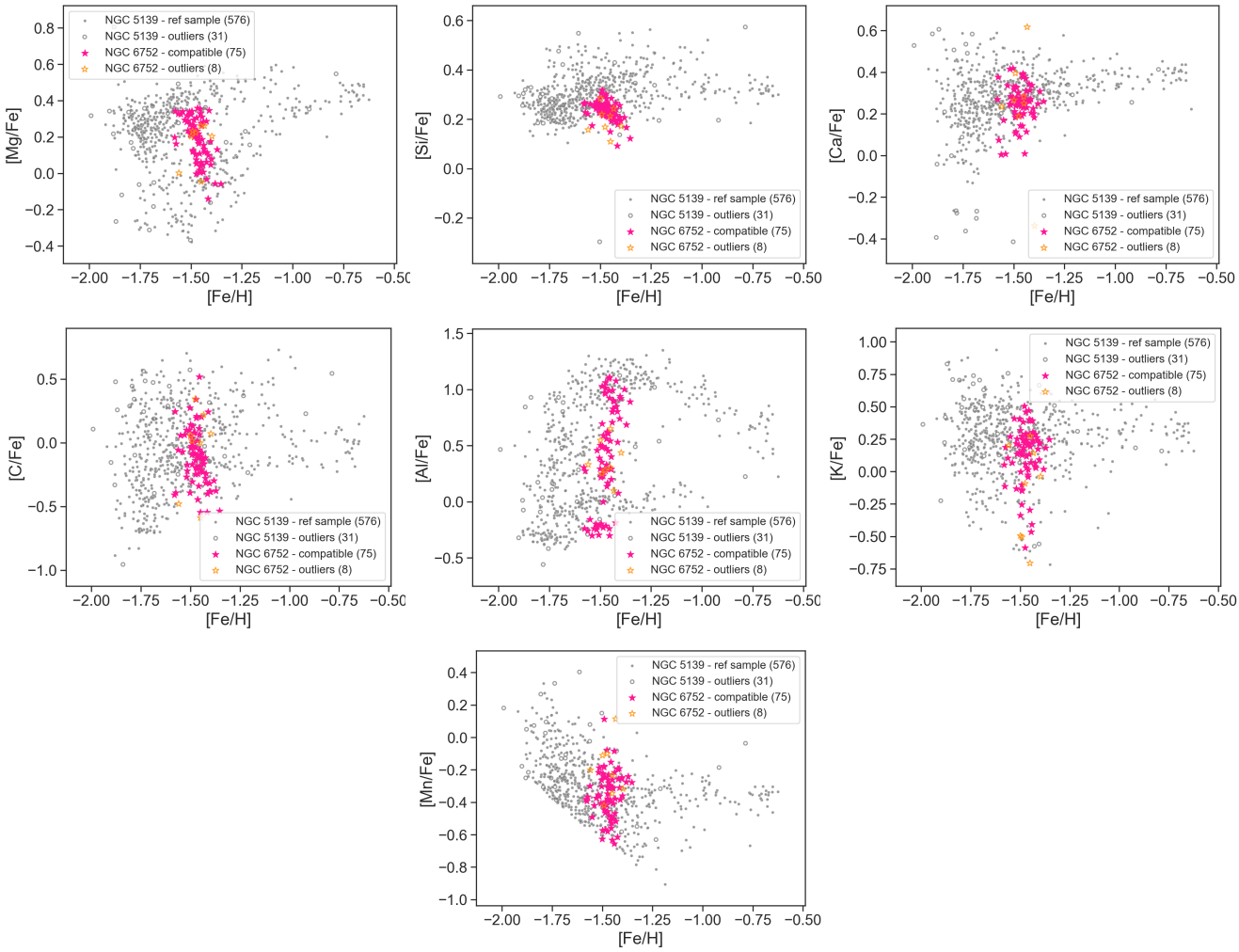

Fig. 3. Same as Fig. 2 but for NGC 6752.

that lead us to classify the clusters chemically compatible with ω Cen into two groups:

1. the first group, consisting of NGC 6656, NGC 6809, and NGC 6273: stars of these GCs are distributed in the abundance spaces in the same regions where the density of ω Cen is highest; that is, these clusters share the chemical properties of most of the stars today in ω Cen. Because, as we shall discuss in Sect. 4.2, the MDF of all these GCs peaks at [Fe/H]$\simeq -1.7$ (see upper row of Fig. 4), in the rest of this paper we shall refer to these GCs as 'metal-poor clusters'.
2. the second group, consisting of NGC 6752, NGC 6205, and NGC 6254: stars of these GCs are distributed in the abundance spaces in regions where ω Cen stars are still present (otherwise, these GCs would not appear as chemically compatible with ω Cen), but in smaller proportions. Their MDF peaks at [Fe/H]$\simeq -1.5$ (see middle row of Fig. 4) and for this reason in the following we refer to these GCs as 'metal-rich clusters'. As we shall discuss in Sect. 4.2, the peak of the MDF of these clusters coincides with one of the secondary peaks of ω Cen MDF, which is often referred to in the literature as one of the 'metal-intermediate' components of ω Cen (RGB-Int1 or MI1 or M-int1, see for example Sollima et al. 2005; Calamida et al. 2020; Alvarez Garay et al. 2024). This group of GCs is in no way associated with the metal-rich population of ω Cen, which is mostly at [Fe/H]$\gtrsim -1$ (see, for example, Alvarez Garay et al. 2024).

Before proceeding with a more detailed description of the characteristics of these clusters in the abundance spaces used, we would like to point out that not all GCs in the metallicity range of ω Cen are chemically compatible with it. For example, NGC 5272, Ter 9, and NGC 3201 have a very low degree of compatibility with ω Centauri (respectively, 11±7, 10±15, and 8±8%, see Table 1), despite the modes and medians of their [Fe/H] distributions being in the range of ω Cen stars – more specifically, in between the first (-1.83 dex) and ninth (-1.31 dex) deciles of the ω Cen MDF. A comparison of the distributions in the [X/Fe] - [Fe/H] spaces of these clusters and ω Cen is given in Sect 4.3.

4.1.1. Metal-poor clusters

Stars of the metal-poor GCs NGC 6656 and NGC 6273 are distributed along a very extended and 'thick'[4] branch in the [Al/Fe]-[Fe/H] plane, and their distributions in the [Mg/Fe], [Si/Fe], [Ca/Fe], [C/Fe], and [K/Fe] versus [Fe/H] planes are visually quite broad. NGC 6809 shows very similar characteristics to the two above-cited clusters, except for the distribution in the [Al/Fe]-[Fe/H] plane, which still is very extended, however not as thick as those of NGC 6656 and NGC 6273. All

[4] By "thick" in this context we mean that the distribution is extended in [Fe/H] at all values of [Al/Fe].

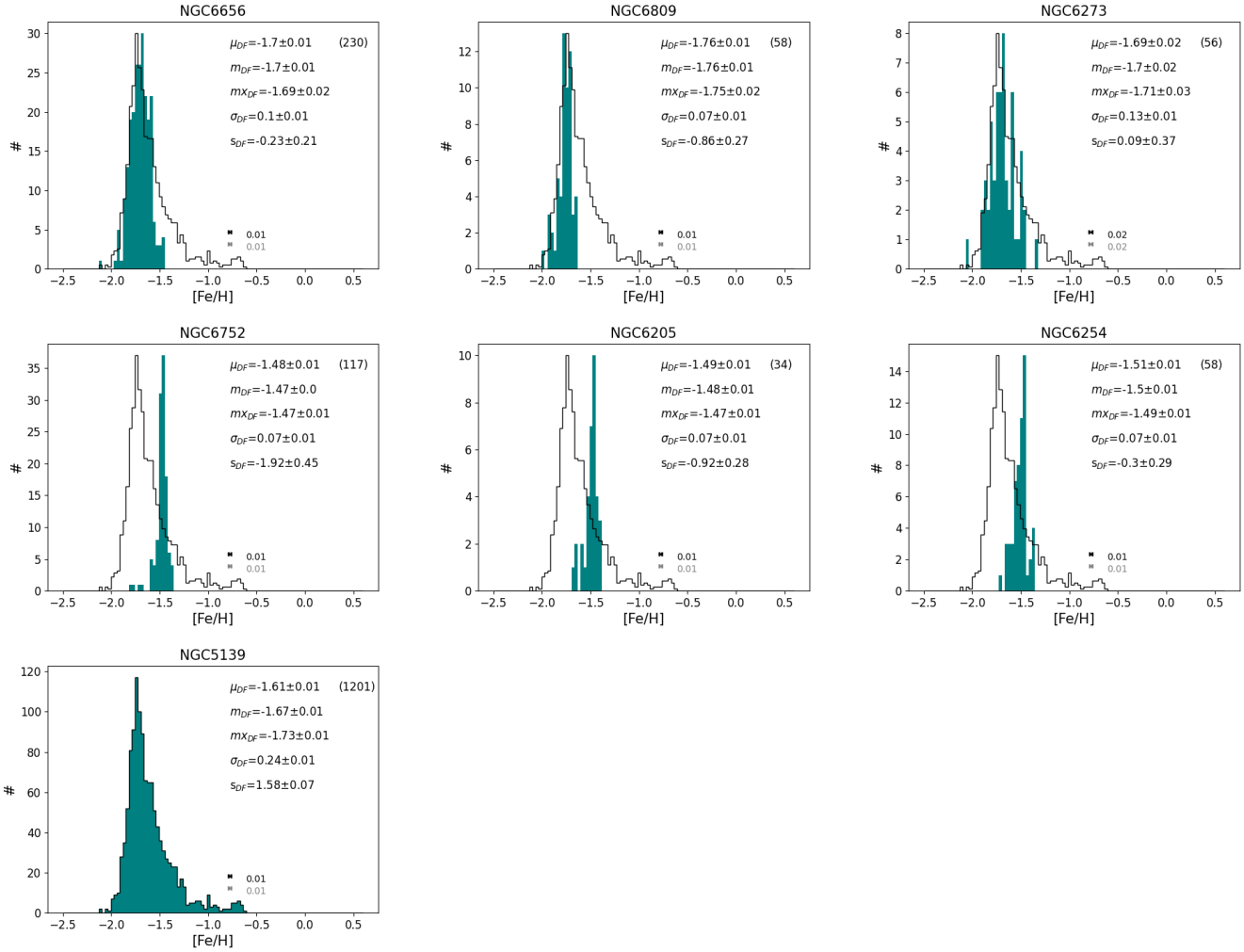

Fig. 4. [Fe/H] distribution of the Galactic globular clusters NGC 6656, NGC 6809, NGC 6273 (the metal-poor clusters, first row), NGC 6752, NGC 6205, and NGC 6254 (the metal-rich clusters, second row), which – according to our analysis – are chemically compatible with ω Cen. For each cluster, the values of the mean, median, mode, dispersion, and skewness of the distribution, and their relative uncertainties, are also reported. The horizontal black and grey error bars at the bottom of each plot show the median and mean uncertainties in [Fe/H], respectively, derived from the Schiavon et al. (2024) catalogue. In each plot, the value reported in parenthesis gives the number of stars used to trace the histogram. For comparison, in each plot, the [Fe/H] distribution of ω Cen (NGC 5139) is also reported (black step-like histogram). The latter has been normalised in such a way that the maximum value coincides with the maximum of the [Fe/H] distribution of the cluster to which it is compared (hence the normalisation varies from plot to plot). The absolute [Fe/H] distribution of ω Cen (i.e. without the normalisation of the peak value) is reported in the last row, with the corresponding mean, median, mode, dispersion, and skewness of its distribution.

these metal-poor GCs appear to have a very extended distribution in the [C/Fe] versus [Fe/H] plane, with a significant fraction of their stars at sub-solar [C/Fe] values, as is expected for red giants during their evolution (see Iben 1967). In NGC 6809, in particular, only a star has a super-solar [C/Fe]. Both the 'thinness' of the distribution in the [Al/Fe]-[Fe/H] plane and the absence of [C/Fe]-rich stars in this cluster may be due to the lower number of stars available for the analysis in this GC (18 – this number rises respectively to 40 and 68, for NGC 6273 and NGC 6656, see Table 1).

ω Cen shows a select number of stars (1.3% of the total) at [Ca/Fe] $\lesssim -0.2$ dex for [Fe/H] values similar to those of the metal-poor GCs. Interestingly, a couple of stars with such low values of [Ca/Fe] are found also in NGC 6656 and NGC 6273, in a proportion similar to that of the [Ca/Fe] deficient population of ω Cen. We note that these stars are classified as outliers by the GMM analysis (empty orange asterisks in Figs. 2 and A.2), since, given the threshold chosen to define the outliers population, stars in ω Cen with similar low values of [Ca/Fe] also end up being outliers (empty grey circles in Figs. 2 and A.2). Among the other α-elements used for the GMM analysis, it is worth commenting on the [Mg/Fe] trends with [Fe/H] for these metal-poor GCs. None of these clusters shows a correlation between the two abundances, except for NGC 6809, which seems to show a decrease in the [Mg/Fe] ratio with increasing [Fe/H] (see top left panel in Fig. A.1). It is worth noting that ω Cen has a fraction of 15% of stars with sub-solar [Mg/Fe] ratios. Except for NGC 6273, for which about 10% of stars has [Mg/Fe] < 0, neither NGC 6656 nor NGC 6809 contains stars with such low values of [Mg/Fe]. Finally, all the metal-poor GCs show the same, nearly flat trend in the [Si/Fe] versus [Fe/H] plane as is observed in ω Cen.

4.1.2. Metal-rich clusters

NGC 6752, NGC 6205, and NGC 6254, the metal-rich clusters, show a number of abundance versus [Fe/H] trends similar

to those found for the metal-poor GCs (see for example the extended distribution in the [Al/Fe]-[Fe/H] plane, which ranges from sub-solar [Al/Fe] ratios to [Al/Fe] ∼ 1 in all three clusters), despite all these GCs being more metal-rich than the previous ones. However, they also show some peculiar features that are worth mentioning:

- a decreasing trend of [Mg/Fe] with increasing [Fe/H], which is particularly prominent in NGC 6752, for which we estimate[5] a Spearman correlation coefficient of −0.42, and a p value of 2×10^{-6}. In this cluster, an anti-correlation is found also for the [Si/Fe] versus [Fe/H] relation (a Spearman coefficient equal to −0.34 and a p value equal to 4×10^{-4}). For NGC 6205 and NGC 6254, milder [Mg/Fe]-[Fe/H] and [Si/Fe]-[Fe/H] anti-correlations are present[6]. For these two GCs, in fact, two trends seem to co-exist: a rising [Mg/Fe] (and [Si/Fe])-[Fe/H] relation (at [Fe/H] $\lesssim -1.55$) and a decreasing one (at [Fe/H] $\gtrsim -1.55$). That is, the trends in [Si/Fe] versus [Fe/H] (but also of [Mg/Fe] versus [Fe/H]) for these clusters are more complex than a simple monotonic description. Besides the strength of the anti-correlations, however, in these clusters the most metal-poor stars[7] have median [Mg/Fe] and [Si/Fe] abundance ratios usually between 0.1 and 0.2 dex greater than those of the most metal-rich stars[8] (see first and second panels, top rows, of Figs. 3, A.3 and A.4).
- both NGC 6752 and NGC 6254 show an extremely [K/Fe]-poor population ([K/Fe] $\lesssim -0.3$ dex) that constitutes less than 10% of the total, and that is also present, at similar [Fe/H] values, in ω Cen.

It is worth mentioning that while we have based the GMM analysis on eight elemental abundances, as is discussed in Sect. 3, the Schiavon et al. (2024) catalogue includes several additional abundance ratios whose analysis allows one to test and indeed strengthen the results presented here. This supplementary discussion is presented in Appendix D (available on Zenodo), both for metal-poor and metal-rich GCs.

Finally, it is also important at this point to clarify an element of nomenclature. In this section, we have sometimes referred to distributions that appear 'broad' in certain [X/Fe] ratios. Obviously, these distributions are not necessarily inherently broad. This depends on the associated ASPCAP uncertainties. We refer the interested reader to Appendix E for an in-depth analysis on [X/Fe] distributions and their intrinsic dispersions, while we discuss the [Fe/H] distributions of the metal-poor and metal-rich clusters below, because – as we shall see – they show interesting similarities between each other and with ω Centauri itself.

4.2. [Fe/H] distributions of globular clusters chemically compatible with ω Cen: Their rise and fall

In this section, we analyse the distribution in [Fe/H] of stars in metal-poor and metal-rich clusters, for which we found a strong chemical compatibility with ω Centauri. Before proceeding with the presentation of this analysis, and the associated discussion, it is necessary to clarify one point. The approach used to establish (or not) a chemical compatibility between the clusters of the Schiavon et al. (2024) catalogue and ω Cen is based on an analysis of the multi-dimensional chemical domain of ω Cen. Once this domain is defined (via the GMM), we define as compatible those clusters for which a high fraction of their stars falls within the ω Cen chemical domain. At no point in this procedure does a density criterion in chemical spaces come into account. That is, it is sufficient for the eight-dimensional pattern of a cluster to be contained in the domain of ω Cen for this cluster to be compatible with it, regardless of the density of this pattern with respect to that of ω Cen itself. At no stage in this procedure, therefore, is it required, for example, that two distributions in chemical abundances – that of a chemically compatible cluster, and that of ω Cen – be similar. Yet, as we shall see below, interesting similarities do exist.

Figure 4 shows the [Fe/H] distributions of the six GCs that are chemically compatible with ω Cen, according to our analysis. For each of these clusters, we report also the mean, median, mode, dispersion, and skewness of the distributions, with their corresponding uncertainties, estimated by bootstrapping all stars of each cluster 100 times, and also taking into account in the bootstrap a Monte-Carlo sampling of the [Fe/H] uncertainties. To draw these distributions, we have included only stars in these six clusters that satisfy the conditions described in Sect. 2 and that have the APOGEE `FE_H_FLAG=0`. In each panel of Fig. 4, we also report the corresponding [Fe/H] distribution of ω Cen stars, re-scaled in such a way that its normalised maximum value coincides with the maximum value of the [Fe/H] distribution of the corresponding GC.

There are several characteristics common to many, sometimes all, of these clusters:

- all of them show total [Fe/H] dispersions, $\sigma_{\rm [Fe/H],tot}$, comprising between 0.07 and 0.13 dex. Given the median of [Fe/H] uncertainties for these clusters, $\epsilon_{\rm [Fe/H]}$, this implies intrinsic [Fe/H] dispersions[9], $\sigma_{\rm [Fe/H],int}$, ranging between 0.07 and 0.12 dex. For the intrinsic [Fe/H] dispersions to be statistically insignificant, this would require median ASPCAP uncertainties in [Fe/H] of the order of $\sigma_{\rm [Fe/H],tot}/\sqrt{2}$ (for median uncertainties, $\epsilon_{\rm [Fe/H]}$, of this order, one would in fact get – by quadrature – comparable values of $\sigma_{\rm [Fe/H],int}$). That is, ASPCAP uncertainties should have been underestimated by a factor, A, between 4 and 5 for the intrinsic dispersions in [Fe/H] to be insignificant (see Table 2 for all these values).
- Three out of six GCs – namely, NGC 6809, NGC 6752, and NGC 6205 – present negatively skewed [Fe/H] distributions, at least at the $>1\sigma$ level. The cases of NGC 6752 and NGC 6809 are particularly remarkable, since the skewness of their [Fe/H] distribution is respectively equal to -1.92 ± 0.45 and -0.86 ± 0.27; that is, the absolute value of the skewness is large and, respectively, nearly five and four times the corresponding uncertainty. A skewness test, performed by making use of the scipy skewtest function[10], confirms that for these three clusters there is a low probability that their [Fe/H] distributions have been drawn from normal distributions (the z scores and p values for these GCs are, respectively: −2.86

[5] By making use of the scipy spearmanr function, see https://docs.scipy.org/doc/scipy/reference/generated/scipy.stats.spearmanr.html

[6] For NGC 6205: Spearman correlation coefficients respectively equal to −0.40 and −0.17, with p values of 0.018 and 0.33; for NGC 6254: Spearman correlation coefficients respectively equal to −0.26 and −0.21, and corresponding p values of 0.05 and 0.12.

[7] Defined as the 1st decile of the distribution.

[8] Defined as the 9th decile of the distribution.

[9] For each cluster, the intrinsic dispersions have been estimated by subtracting the median of the measurement uncertainties, $\epsilon_{\rm [Fe/H]}$, in quadrature.

[10] https://docs.scipy.org/doc/scipy/reference/generated/scipy.stats.skewtest.html#scipy.stats.skewtest

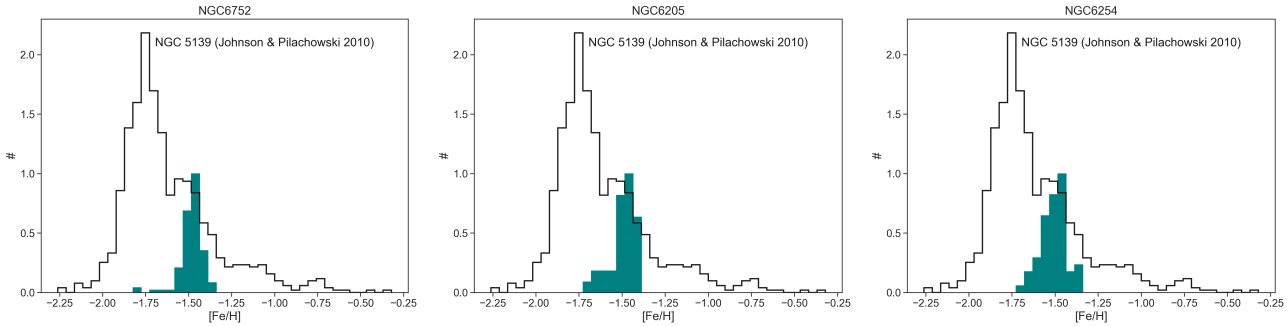

Fig. 5. [Fe/H] distribution of the metal-rich GCs that are chemically compatible with ω Cen; namely NGC 6752, NGC 6205, and NGC 6254. For comparison, in each plot, the [Fe/H] distribution of ω Cen (NGC 5139) reported in Johnson & Pilachowski (2010) is also shown (black step-like histogram). The latter has been normalised in such a way that the secondary peak value coincides with the maximum of the [Fe/H] distribution of the cluster to which it is compared.

Table 2. Total and intrinsic [Fe/H] dispersions for the metal-poor and the metal-rich GCs chemically compatible with ω Centauri.

GC name	# stars	$\sigma_{[Fe/H],tot}$	$\epsilon_{[Fe/H]}$	$\sigma_{[Fe/H],int}$	A
NGC 6656	230	0.10	0.01	0.10	5.36
NGC 6809	58	0.07	0.01	0.07	4.29
NGC 6273	56	0.13	0.02	0.12	5.18
NGC 6752	117	0.07	0.01	0.07	4.13
NGC 6205	34	0.07	0.01	0.07	4.05
NGC 6254	58	0.07	0.01	0.07	4.18
NGC 5139	1201	0.24	0.01	0.24	12.87

Notes. For each cluster, we also report the median of the [Fe/H] uncertainties of its stars, $\epsilon_{[Fe/H]}$, and the factor A by which these uncertainties would have to be underestimated for the intrinsic dispersions not to be statistically significant. The same quantities for ω Cen (NGC 5139) are also reported.

and 0.004, −6.66 and less than 0.0001, −2.44 and 0.014)[11]. Two clusters, NGC 6656 and NGC 6254, have marginally skewed MDFs, at a level of $\sim 1\sigma$[12], while NGC 6273 is the only GC with a skewness compatible with 0, given the corresponding uncertainty.

– the significant negative skewness of the [Fe/H] distribution of the above-cited GCs reflects a characteristic shape, with an initial rise in the number of stars at a given [Fe/H] for increasing values of [Fe/H], followed by a sharp truncation at the highest [Fe/H] values. This behaviour is found for all metal-rich GCs and for one of the metal-poor GCs; namely, NGC 6809.

About metal-poor GCs, it is very interesting to note that:

1. all of them have an MDF peak coinciding with the peak of the ω Cen MDF;
2. the rising part of their MDF is comparable to the rising part of the (normalised) MDF of ω Cen (compare the dark green and black step-like histogram in the top row panels of Fig. 4).

These two findings indicate that the rate of iron formation in these GCs and in ω Cen was the same until these GCs and ω Cen itself reached a maximum (corresponding to the peak of their MDF), after which a more or less rapid decrease in iron production follows.

Among metal-rich GCs, it is interesting to note that:

1. their MDFs peak at the same [Fe/H] value, given the uncertainties;
2. their most metal-poor stars have metallicities similar to those at the peak of the ω Cen MDF (at about [Fe/H] $\simeq -1.73$).

By assuming the metallicity as a measure of time, these two findings could suggest that these clusters started forming when the star formation and metal production in ω Cen was at its maximum and that in all of them, the star formation ceased at the same time. Additional investigation will be needed to confirm or reject this scenario (see also Sect. 5 for a discussion of the ages of these clusters).

With regard to the population of metal-rich GCs, it is interesting to further investigate the comparison with the MDF of ω Cen stars. Several works indeed report that, in addition to the primary peak at [Fe/H] ~ -1.7 dex, the MDF of ω Cen has a series of secondary peaks, one of which at [Fe/H] ~ -1.5 dex (see, for example Johnson & Pilachowski 2010; Alvarez Garay et al. 2024). This secondary peak is not clearly visible in the APOGEE data, possibly due to the spatial coverage of the ω Cen stars observed by APOGEE, with a deficiency of stars in the central regions of the cluster (see Figs. 10 and 11 in Alvarez Garay et al. 2024). In Fig. 5, we compare the MDF of ω Cen, derived from the data of Johnson & Pilachowski (2010), with that of the group of metal-rich clusters that we have identified as chemically compatible with it. The comparison is striking: these three GCs all have MDFs that peak where the secondary maximum of the ω Cen MDF is located.

The two groups of clusters found therefore have peaks that coincide with either the primary peak of metallicity of ω Cen or with its secondary peak. This result is not a consequence of the method we used to quantify the chemical compatibility between the clusters in question and ω Cen (see introduction to this section). It is rather proof that the similarity between these clusters and ω Cen is not coincidental. Indeed, for a cluster to be chemically compatible with ω Cen it is sufficient that it falls within its chemical domain, but its mean (or median or mode) metallicity could be any value contained between ω Cen's minimum and maximum metallicity. That is, there is no reason for the

[11] Note that NGC 6752 has four stars with [Fe/H] < −1.65 that, when removed, obviously imply a decrease in the [Fe/H] dispersion (which decreases from 0.07 to 0.05) and skewness (which increases from −1.92 to −0.17). However, after checking their proper motions and radial velocities, these stars appear to be typical of the cluster and we could not find any particular reason to disregard them

[12] For these two GCs, the skew test is also not conclusive, since it results in z scores and p values equal, respectively, to −1.43 and 0.15 (for NGC 6656) and −1.25 and 0.21 (for NGC 6254).

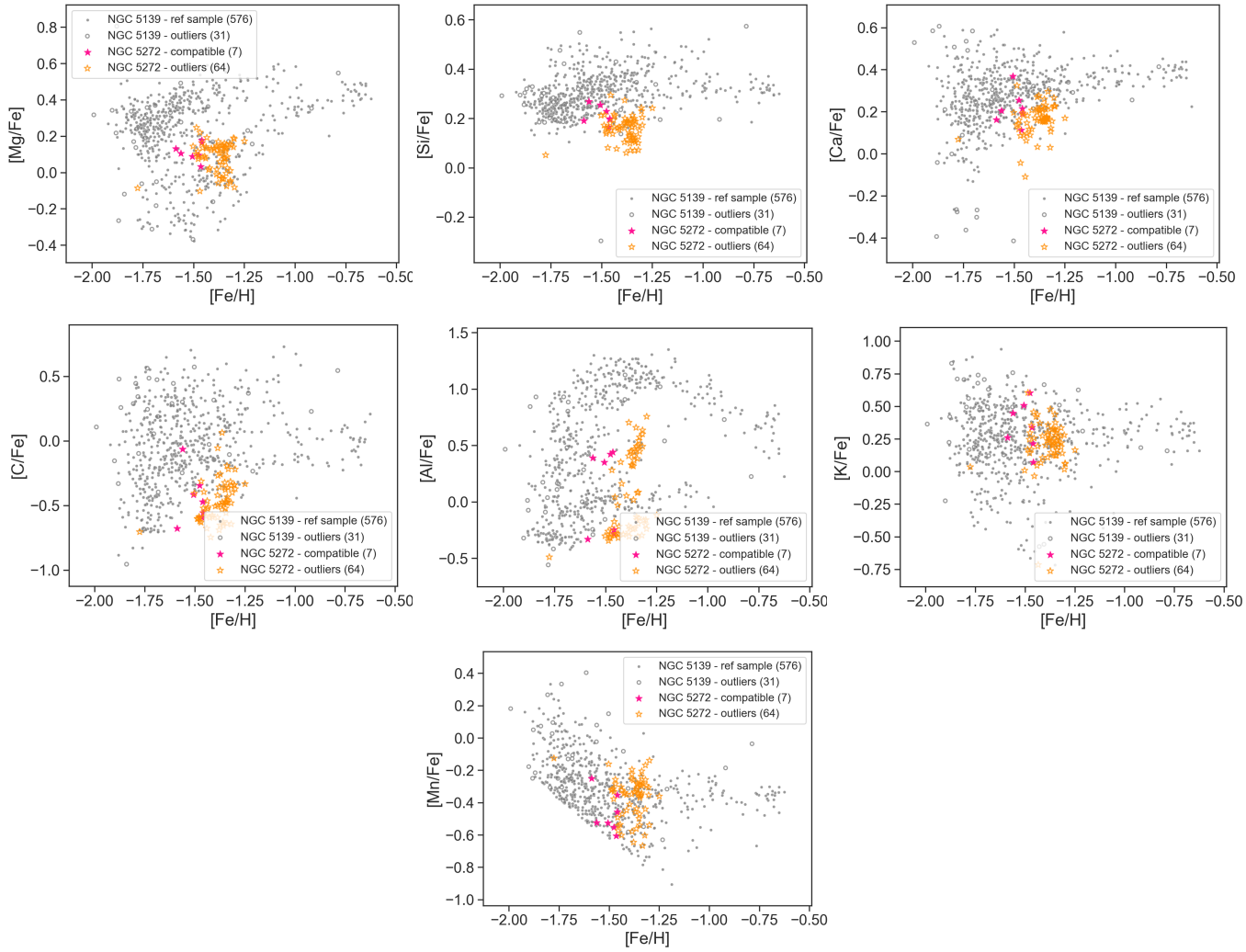

Fig. 6. Chemical abundance relations for members of NGC 5272 (colour) and ω Cen (grey). The filled symbols show the reference sample of ω Cen (grey) and the stars of NGC 5272 (magenta) chemically compatible with it according to the GMM (see Sect. 4), while the empty ones (grey and orange colours) correspond to their outliers. The number of stars in each category is reported in parentheses. NGC 5272 is an example of a GC in the metallicity interval of ω Cen, which has a very low chemical compatibility with it (see also Appendix B, available on Zenodo).

metallicities of compatible clusters to clump into two distinct groups, which in addition overlap with the two main metallicity peaks of ω Cen itself. These similarities in the MDFs of these clusters is thus a posteriori additional confirmation of the relevance of our findings, and allow us to strongly anchor NGC 6752, NGC 6205, and NGC 6254 to ω Cen and its progenitor galaxy.

4.3. Whether all stellar systems in the range of ω Cen metallicities have similar chemical patterns

Previous results have allowed us to show the existence of a group of GCs with the same chemical patterns found within the ω Centauri cluster. We looked into whether such a result is obvious; in other words, whether this similarity is simply due to the fact that, at the metallicities of ω Cen, all clusters have similar chemical compositions.

Among the clusters listed in Table 1, clusters like NGC 5272, Ter 9, and NGC 3201 have a very low fraction of stars compatible with ω Cen, despite being in its metallicity range. Abundance ratios for these clusters, as a function of [Fe/H], are shown in Fig. 6 (and in Appendix B, available on Zenodo). In these figures, similar to what is shown in Figs. 2 and 3, for each cluster both stars that the GMM classifies as compatible with ω Centauri (magenta symbols) and the outliers (orange symbols) are shown. As can be seen, for all these clusters, some chemical patterns (e.g. [Mg/Fe] vs. [Fe/H], [K/Fe] vs. [Fe/H]) overlap with those of ω Cen, while others (e.g [Si/Fe] vs. [Fe/H], or [Ca/Fe] vs. [Fe/H], or [C/Fe] vs. [Fe/H]) do not. Thus, when a sufficient number of chemical abundances are used, differences between clusters emerge, even for clusters that have similar metallicities. This shows that the chemical compatibility found between NGC 6656, NGC 6273, NGC 6809, NGC 6254, NGC 6205, and NGC 6752 and ω Cen is not merely the result of the fact that at these metallicities all GCs should resemble each other. NGC 5272, Ter 9, and NGC 3201 are indeed proof that differences in the chemistry of stellar systems can be found even at these metallicities. The chemical compatibility of NGC 6656, NGC 6273, NGC 6809, NGC 6254, NGC 6205, and NGC 6752 and ω Cen, combined with the common characteristics of their MDFs discussed above, is rather proof that these clusters share the same formation environment, which is different from that of other Galactic GCs with similar metallicities.

Not only are there GCs in the metallicity range of ω Cen that are not chemically compatible with it. By comparing the

Table 3. Fraction of stars in the most massive satellites of the MW (LMC, SMC, Sagittarius, and Fornax) chemically compatible with ω Cen.

Satellite	[Fe/H] < −1	[Fe/H] < −1.3	[Fe/H] < −1.5
LMC	4% (8 out of 211)	13% (8 out of 62)	32% (8 out of 25)
SMC	0% (0 out of 322)	0% (0 out of 40)	0% (0 out of 14)
Sgr	4% (2 out of 81)	6% (2 out of 34)	25% (2 out of 8)
Fnx	0% (0 out of 43)	0% (0 out of 6)	0% (0 out of 2)

Notes. This fraction has been estimated for three different [Fe/H] intervals, reported in the different columns.

chemical patterns of the most massive MW satellites – namely, the Large Magellanic Cloud (LMC), Small Magellanic Cloud (SMC), Sagittarius (Sgr), and Fornax (Fnx) – for which data are available in APOGEE DR17, we can quantify their degree of compatibility with ω Cen, applying the same procedure used for the GCs. For these galaxies, we used the APOGEE data presented in Hasselquist et al. (2021). In particular, their Table 2 provides the identifiers of stars belonging to these galaxies, which we cross-identified with the APOGEE DR17 catalogue to obtain their chemical abundances. From the retrieved sample, for the LMC, SMC, and Sag, we then selected only stars with:

1. a signal-to-noise ratio of `SNREV` > `70`;
2. temperatures in the range of 3500 K < T_{eff} < 5500 K and surface gravities of log g < 3.6;
3. `APOGEE STARFLAG and APOGEE STARBAD` = `0.`

For Fornax, we applied less strict selection criteria than those used above, and made use of all Fornax stars in Hasselquist et al. (2021), in order to keep stars at [Fe/H] < −1. As for NGC 5139 (ω Cen), we used the Schiavon et al. (2024) catalogue, applying the same selections discussed in Sect 2.

By making use of the same eight-dimensional space of chemical abundances used for the analysis of GCs, in Table 3 we report the fraction of stars in these galaxies that are chemically compatible with ω Cen, for different cuts in metallicity. Even for the most restrictive cuts, where we limit the analysis only to stars with [Fe/H] lower than −1.5, we see that the fraction of stars of these galaxies compatible with ω Cen chemistry is 32%, at the most (see Appendix F, available on Zenodo, for the corresponding plots). That is, none of the aforementioned dwarf galaxies is chemically compatible with ω Cen, in its range of metallicities. This result has two implications:

1. the progenitor galaxy of ω Cen must have had a different chemical evolution from that which LMC, SMC, Sagittarius, and Fornax had, at the same metallicities;
2. the chemical non-compatibility of ω Cen with LMC, SMC, Sagittarius, and Fornax also implies the chemical incompatibility of NGC 6656, NGC 6273, NGC 6809, NGC 6254, NGC 6205, and NGC 6752 with them. We can therefore exclude that these GCs formed in galaxies that had similar chemical evolution to the most massive satellites of the MW, at the same metallicities.

4.4. Orbital properties of globular clusters chemically compatible with ω Cen

Once clusters chemically compatible with ω Cen have been identified on the basis of their abundances only, it is interesting to go back to kinematic spaces and investigate their orbital properties. To estimate the orbital parameters, we made use of the publicly available code `galpy` (Bovy 2015), adopting the McMillan (2017) Galactic potential. The positions and proper motions of all Galactic GCs and field stars studied in this section are taken from *Gaia* EDR3 data, whilst the radial velocities are taken from APOGEE DR17. The distances are the ones generated by Leung & Bovy (2019b) for the APOGEE DR17 catalogue, using the `astroNN` python package (see Leung & Bovy 2019a). These distances were determined using a re-trained `astroNN` neural-network software, which predicts stellar luminosity from spectra using a training set comprising stars with both APOGEE DR17 spectra and *Gaia* EDR3 parallax measurements. We used a right-handed Galactocentric frame that leads to a three-dimensional velocity of the Sun equal to $[U_\odot, V_\odot, W_\odot] = [11.1, 248.0, 8.5]\,\mathrm{km\,s^{-1}}$ (Horta et al. 2023). We assumed the distance between the Sun and the Galactic centre to be $R_\odot = 8.178$ kpc (GRAVITY Collaboration 2019), and the vertical height of the Sun above the midplane to be $z_\odot = 0.02$ kpc (Bennett & Bovy 2019).

Figure 7 shows the distribution in the E – L_z and L_{perp} – L_z spaces of our sample of GCs in comparison to field stars in APOGEE DR17. These are the two kinematic spaces most commonly used in the literature to derive the origin of Galactic GCs, where E is the total orbital energy, L_z is the z component of the angular momentum space in a reference frame with the Galactic disc in the xy plane, and L_{perp} is the projection of the total angular momentum onto the Galactic plane. The bottom panel of Fig. 7 shows the distribution of all Galactic GCs (with at least 15 stars) in the Schiavon et al. (2024) catalogue in the $E - L_z$ plane (left panel) and in the $L_{perp} - L_z$ plane, in comparison to all field stars in the APOGEE DR17 catalogue. For the GCs, the values of energies and angular momenta reported in these panels are the mean values, averaged over all stars that have a high probability of being members of each cluster (see Sect. 2). In the same panel of Fig. 7, clusters are colour-coded according to the fraction of their stars compatible with ω Cen, as is listed in Table 1. We can see that GCs with a high fraction of stars chemically compatible with ω Cen are distributed over an extended region of these kinematic planes and are mixed with GCs with a lower fraction. The upper panel of Fig. 7 focusses on the E – L_z and L_{perp} – L_z of GCs for which at least 60% of the stars are chemically compatible with ω Cen in comparison to the other GCs in the sample and the field stars in APOGEE DR17. As we can see, these GCs occupy a large region in the kinematic diagrams due to the uncertainties on these quantities and the cluster's intrinsic velocity dispersion. In fact, the more massive the cluster, the greater its dispersion, as we can see from the ω Cen extension in the kinematic spaces. Despite this, we can clearly see that the GCs that are chemically compatible with ω Cen have different kinematic properties, spanning a wide range of L_z ($-10^3\,\mathrm{kpc\,km/s} \lesssim L_z \lesssim 10^3\,\mathrm{kpc\,km/s}$) and E ($-2.1 \times 10^5\,(\mathrm{km/s})^2 \lesssim E \lesssim -1.6 \times 10^5\,(\mathrm{km/s})^2$). In particular, we emphasise the fact that ω Cen and NGC 6205 appear to have a retrograde orbit, while the other compatible clusters have both prograde orbits (NGC 6656 and NGC 6752) and orbits with $L_z \sim 0$ (NGC 6273, NGC 6809, and NGC 6254). In particular, it is interesting to note that the clusters most compatible with ω Cen – namely, NGC 6752 and NGC 6656 – are actually the most prograde, meaning that the kinematic criteria would suggest they are not associated with ω Cen.

Given the wide spread found in energy and angular momenta for GCs chemically compatible with ω Cen, it is questionable whether it is realistic to imagine a common origin for them. In Fig. 8, we show the simulated distribution in energy and angular momenta of a set of ten clusters, accreted, together with their progenitor galaxy, on a MW-type galaxy. This simulation is one

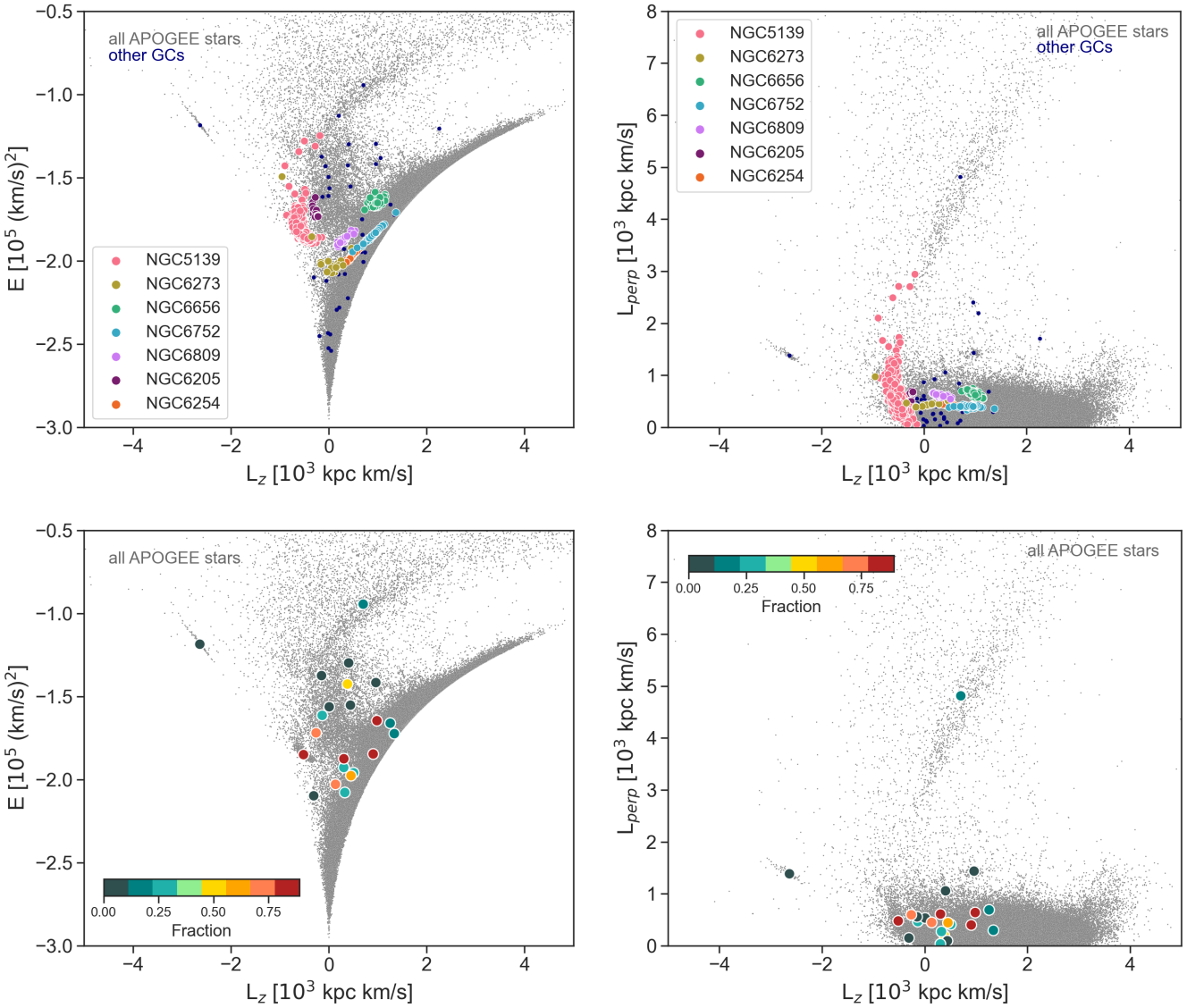

Fig. 7. Distribution of GCs and field stars in kinematic spaces: orbital energy (E) and projection of the total angular momentum onto the Galactic plane (L_{perp}) vs. the z component of the angular momentum (L_z). Top panel: star-by-star distribution in the E – L_z and L_{perp} – L_z spaces of GCs for which at least 60% of the stars are chemically compatible with ω Cen. Other GCs in our sample are shown as blue points (mean values). Bottom panel: distribution in the E – L_z and L_{perp} – L_z spaces of GCs, which are colour-coded according to the fraction of stars that are chemically compatible with ω Cen (see Table 1). Only GCs with a total number of stars greater than 15 are shown. For comparison, in both panels, the distribution of all APOGEE stars is shown as grey points. Note that the sign of L_z has been inverted from the usual sign of L_z in a right-handed system to enable a better comparison with other works in the literature.

of those presented in Pagnini et al. (2023) (identified in that paper with the ID=MWsat_n1_Φ180). In this simulation, the orbital plane of the satellite is initially inclined by 180 degrees with respect to the disc of the MW-type galaxy – meaning that the orbit is initially retrograde in the plane of the MW-type galaxy – and the mass of the satellite is one tenth of that of the MW. In Fig. 8, energies and angular momenta have been re-normalised in order to obtain a distribution comparable with that of the Galactic GCs and field stars presented in the previous figure. For this, we have multiplied positions, velocities, and masses, respectively, by factors of 1.89, 1.06, and 2.12, which implies also re-scaling the timescale by a factor of 1.79, to keep the virial ratio = 1. We emphasise that this simulation does not intend to provide the most probable scenario for the accretion of ω Cen and its related GCs in the MW, and therefore neither the mass ratio nor the orbital parameters used in this simulation should be taken literally as representative of this accretion history. Incidentally, no NSC is included in the simulated satellite. This simulation simply serves us to show that, even in the case of an initially retrograde orbit, a sufficiently massive accretion on a MW-type galaxy can lead to accreted clusters on prograde orbits similarly to what is shown in Fig. 7. An interesting point emerging from this simulation is that a number of accreted GCs are found on retrograde orbits at high energy levels (at $E \gtrsim -1 \times 10^5$ (km/s)^2). These high-energy GCs are those, in the simulations, lost by the satellite in the early phases of its accretion. This is a region not probed by the GCs data used for this work, so it is not possible for us to test whether GCs chemically compatible with ω Cen are also present at these energy values, but it would be extremely interesting to conduct such kind of analysis in the future, once sufficient spectroscopic data is available, because – if found – the location of these high-energy GCs

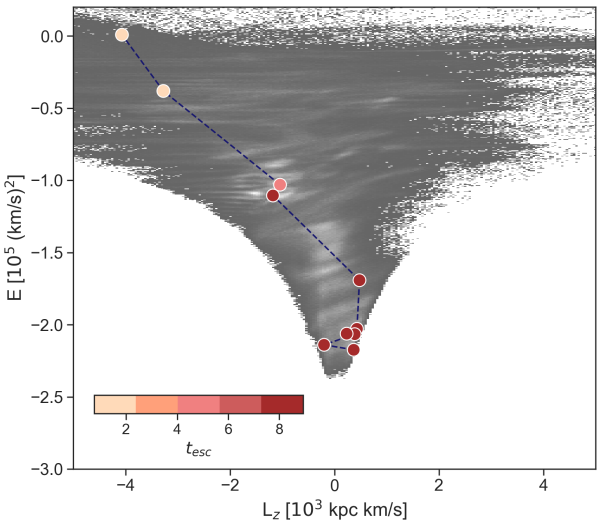

Fig. 8. Distribution in E – L$_z$ of a set of ten clusters accreted together with their progenitor galaxy on a MW-type galaxy through one of the *N*-body simulations presented in Pagnini et al. (2023) (identified in that paper with the ID=MWsat_n1_Φ180). Clusters are colour-coded according to their escape time from the progenitor satellite, which is defined as the time when the distance between the GC and the satellite's centre of mass is larger than 15 kpc (see Sect. 3 in Pagnini et al. 2023 for the details). In the background, the distribution of field stars of the accreted satellite is also shown as a density map. Energies and angular momenta have been re-scaled to obtain a distribution comparable with that of the Galactic GCs and field stars presented in Fig. 7.

in the $E - L_z$ plane may help to constrain the early history of this accretion.

5. Discussion

The chemical similarity between ω Cen and some of the clusters discussed in this paper has already been studied and emphasised in the literature. The first comparison, to our knowledge, of chemical abundances in ω Cen, NGC 6656 (M 22), and NGC 6752 was presented by Norris & Freeman (1983), who, after comparing CN, Ca, and Al in these three clusters, suggested 'common abundance enhancement mechanisms which increase in degree in going from NGC 6752, through M 22, to ω Cen'. The high levels of carbon enhancement found in ω Cen and NGC 6656, but not in NGC 6752, led the authors to point out the exceptionality of the former two GCs with respect to NGC 6752 and other, more normal, clusters.

Extensive work has been presented in more recent years on the chemical peculiarities and abundance variations in NGC 6656 (see, for example, Marino et al. 2009; McKenzie et al. 2022) and the striking similarities with ω Cen (Da Costa & Marino 2011; Marino 2015). In particular, Da Costa & Marino (2011) provided a number of elements of comparison between the two clusters, and it is worth discussing here the similarities and differences between our conclusions and interpretations and those presented in their paper.

One of the first striking similarities between ω Cen and NGC 6656 is, of course, the discovery of a significant iron spread in both of them. While the existence of an iron spread in ω Cen has been known for quite a long time now (see introduction), the discovery of a spread in Fe-content in NGC 6656 is more recent (Da Costa et al. 2009; Marino et al. 2009, but see also Pilachowski et al. 1982; Lehnert et al. 1991 for earlier evidence of Fe-variations in this cluster). Since then, this discovery has been subject to some debate (see, for example Mucciarelli et al. 2015; Bailin 2019; Mészáros et al. 2021; McKenzie et al. 2022, and, in particular, Table 1 in this latter work for a summary of the publications on this matter). Figure 1 in Da Costa & Marino (2011) shows the comparison between the [Fe/H] distribution of ω Cen and that of NGC 6656, based on which the authors emphasise a considerable degree of similarity between these two clusters. They indeed observe that both distributions rise rapidly on the metal-poor side to a well-defined peak, which, however, they find to differ by about 0.09 dex (the peak in the NGC 6656 MDF results is more metal-poor than that in ω Cen). Our analysis confirms Da Costa & Marino (2011)'s findings, and allows us to push these similarities between the two MDFs even further: indeed the two peaks result mostly superposed, with the MDF of ω Cen peaking at [Fe/H]= -1.73 ± 0.01 and that of NGC 6656 peaking at [Fe/H]= -1.69 ± 0.02. Moreover, the rate of increase on the metal-poor side of the MDF is also impressively similar, as is discussed in Sect. 4.2. The higher difference found by Da Costa & Marino (2011) in the location of the peaks compared to ours may be due to the way the [Fe/H] distribution for ω Cen was derived in their work (from the [Ca/H] distribution presented in Norris et al. 1996, by assuming a constant [Ca/Fe] ratio of 0.4 dex, see details in their paper).

Concerning α elements, we confirm what already discussed by Da Costa & Marino (2011) about the lack of Mg-depleted stars in NGC 6656, which are instead present, at similar metallicity values, in ω Cen (see Fig. 2). Some Mg-depleted stars are, however, present in another of the metal-poor clusters chemically compatible with ω Cen: NGC 6273, which is also a cluster strikingly similar to ω Cen in many aspects, as was shown in the previous sections, and which shares, with NGC 6656, the same similarities to ω Cen as for their MDFs. While NGC 6656 does not show, in the current data, any presence of Mg-depleted stars, it does show the presence of a few Ca-depleted stars, another characteristic found also in NGC 6273 as well as in ω Cen itself (see Figs. 2 and A.2). The similar abundance patterns shared by ω Cen, NGC 6656, and NGC 6273 have also been investigated by Johnson et al. (2015), who point out, among other similarities, that the shape and slope of the [La/Fe] and [La/Eu] distributions are nearly identical in all these clusters (see also Johnson et al. 2017, for further analysis).

Of the three metal-poor GCs chemically compatible with ω Cen, NGC 6809 is the only cluster for which we could not find in the literature any direct comparison of its abundances with those of ω Cen. NGC 6809 is actually considered a 'normal' cluster, with the usual light-element variations found in other clusters, but with no iron spread (Carretta et al. 2009; Rain et al. 2018, but see also Bailin 2019 who reported a small, but nonzero spread for this cluster). We do find an iron spread in the APOGEE data, which is significant, given the uncertainties on the [Fe/H] estimates reported in the catalogue (for further details, see discussion in Sect. 4.2). In this regard, it is interesting to note that in the work by Rain et al. (2018), based on the abundance analysis of a sample of 11 red giant branch stars in NGC 6809, a star with a difference of −0.2 dex compared to the average iron content is reported[13]. To explain the presence of such a star, the authors evoke the possibility that it could be a pulsating variable (but note that, as the authors themselves acknowledge, they lack the photometry necessary to probe the statement). While this possibility cannot be ruled out, it is also possible that the iron content of this star is intrinsically different

[13] Note that this star was removed by Bailin (2019) in estimating the spread of NGC 6809.

from the rest of the stars analysed in their work. We do also find a star in NGC 6809 with a [Fe/H] of −0.2 dex lower than the average value for the cluster, which represents 2% of our NGC 6809 sample. As we checked, this ratio rises to 14% for stars with a difference of −0.1 dex compared to the average iron content of the cluster.

As for the metal-rich clusters chemically compatible with ω Cen, we have already reported the early work by Norris & Freeman (1983), who emphasised a common abundance enhancement mechanism increasing in strength from NGC 6752 to ω Cen. The lack of stars in NGC 6752 as Ca-enhanced as in ω Cen led the authors to consider the similarity between the two clusters with some caution. Our analysis confirms that ω Cen contains stars with [Ca/Fe] > 0.5 dex; these are rare in NGC 6752, but still one of the 83 stars in our sample shows such a high Ca content (see Fig. 3). However, it is important to emphasise that ω Cen stars with extreme Ca abundances are found for [Fe/H] $\lesssim -1.6$ dex, so essentially at metallicities lower than those spanned by NGC 6752 stars. Coming back to Fig. 3, it is indeed striking to see that NGC 6752 stars do cover the entire [Ca/Fe] range spanned by ω Cen at similar metallicities (note in particular the presence of a Ca-depleted star with a [Ca/Fe] ratio similar to those found for the (rare) Ca-depleted population present in ω Cen, as well as the presence of the stars with [Ca/Fe] > 0.5 dex, already mentioned above). As for the iron spread, we do find one, even if smaller than the spread found for clusters such as NGC 6656 or NGC 6273. A weak iron spread for NGC 6752 was also reported by Yong et al. (2013).

The fact that different clusters have chemical patterns also observed in ω Cen should not be surprising in itself. One hypothesis for the formation of NSCs is that they are the product of the orbital decay of GCs in the central regions of their galaxy (e.g. Tremaine et al. 1975; Capuzzo-Dolcetta 1993; Antonini et al. 2012, 2015; Mastrobuono-Battisti et al. 2014; Gnedin et al. 2014; Perets & Mastrobuono-Battisti 2014; Arca-Sedda et al. 2015; Tsatsi et al. 2017; Abbate et al. 2018). Thus, finding the imprint of GCs in a NSC is in itself a result in line with one of the theoretical hypotheses for the formation of these systems. This would be, to our knowledge, the first time that such a correspondence has been highlighted in observational data and this in itself constitutes an important result of our study (see Alfaro-Cuello et al. 2019, 2020; Kacharov et al. 2022, for a similar conclusion on M54). In this scenario, clusters with chemical patterns similar to those of NGC 6656, NGC 6273, NGC 6809, NGC 6205, NGC 6254, and NGC 6752 would have decayed into the centre of the progenitor galaxy of ω Cen, forming part (at least the metal-poor part) of it. However, this hypothesis does not fully represent what we find, or rather, what we find seems to indicate a more global scenario, which this hypothesis alone cannot explain. For example, the question of why clusters 'that decayed' in the inner regions of the progenitor galaxy should share such chemical similarities. In this scenario, it would have been sufficient to find a few clusters chemically compatible with ω Cen, but what our data show is that not only is each of these GCs chemically compatible with ω Cen, but they all share some important chemical similarities.

Indeed, beyond the individual comparison of each cluster with ω Cen, what our analysis reveals is that all these clusters have properties in common. The similarities of the MDF of the metal-poor clusters, on the one hand, and of the metal-rich clusters, on the other, reveal that these groups of clusters have similar global properties, which point to a formation and an early evolution tightly linked to that of their environment (i.e. the progenitor galaxy itself or part of it). For example: (1) the similarities in the rising part of the MDFs of NGC 6656, NGC 6273, NGC 6809, and ω Cen itself point to a simultaneous origin of these clusters, which must have experienced a similar star formation in the early phases of their evolution; (2) the similarities in the MDF of NGC 6205, NGC 6254, and NGC 6752 suggest a formation that started, reached its maximum, and ceased at the same time in these clusters and that is moreover clearly linked to one of the populations found in ω Cen (i.e. the intermediate 1 population, see for example Sollima et al. 2005; Calamida et al. 2020; Alvarez Garay et al. 2024); (3) the correlation found in the [Mg/Fe]-[Fe/H] and in the [Si/Fe]-[Fe/H] plane for these three clusters may suggest that the ISM in which these GCs formed was being enriched by type Ia supernovae (SNe Ia), and that possibly the star formation process went on for some time, in order to produce the declining [Mg/Fe] and [Si/Fe] ratios with [Fe/H] found in these clusters[14]. The possibility that SNe Ia may play a role in the star formation and chemical enrichment of Galactic GCs has recently been addressed by means of three-dimensional hydrodynamical simulations by Lacchin et al. (2021). Interestingly, some of their models (those in which SNe Ia ejecta are retained by the cluster, and mix with AGB ejecta and with high-density gas accreted by the cluster during its motion in the galaxy) produce negatively skewed metallicity distributions (see Figs. 10 and 11 in their paper), as we find for NGC 6205, NGC 6254, and NGC 6752.

It is also interesting to comment on the ages of these two groups of clusters. The three metal-rich GCs and two out of three metal-poor GCs had their ages measured in Marín-Franch et al. (2009) and VandenBerg et al. (2013). In Marín-Franch et al. (2009), the three metal-rich GCs were found to belong to the 'young' GC group, while the two metal-poor GCs belong to the old group classification introduced by these authors, with an overall age difference of about 1 Gyr. Similarly, VandenBerg et al. (2013) found an age of 12.00, 11.75, and 12.50 Gyr for NGC 6205, NGC 6254, and NGC 6752, respectively, and 12.50 and 13.00 for NGC 6656 and NGC 6809. There is, then, a consistent indication of an age difference between the metal-poor and metal-rich groups, suggestive of a possible chemical enrichment with time from one group to the other. Whether this is compatible with a corresponding evolution in ω Cen remains to be clarified given the complexity of the relation between age and metallicity in this system.

The common chemical abundance properties of these clusters (with each other and with ω Cen) also lead us to rule out the possibility that these clusters are the NSCs of galaxies that have been accreted in the past by the MW. This is one of the most accepted hypotheses to explain the origin of clusters with high metallicity spreads, including NGC 6656 and NGC 6273 (see, for example Da Costa 2016; Pfeffer et al. 2014, 2021). While we think that among the clusters proposed by Da Costa (2016) some are indeed NSCs of dwarf galaxies – besides ω Cen and NGC 6715, NGC 2808 is another interesting case that deserves additional investigation (see Lardo et al. 2023) – we believe that NGC 6656 and NGC 6273 are not ancient NSCs of galaxies, for the following reasons:

– The chemical similarities of these clusters with each other and with ω Cen, and the similar properties of their MDFs, would imply that they were formed in galaxies with a strikingly similar chemical evolution. These elements would be difficult to explain if they were truly independent systems.

[14] Note that we have checked that this trend is robust, that is it does not depend either on the surface gravity nor on the effective temperature of the analysed stars.

– Among the clusters whose chemical compatibility with ω Cen we have quantified, there is NGC 6715 (M54), which is believed to be the NSC of the Sagittarius dwarf galaxy. The comparison between ω Cen and the latter shows very low chemical similarity (at the 16% level, see Table 1), which for us reinforces the argument that NSCs formed in different galaxies should have different chemical properties. As a further check, we applied the GMM restricting only to the metallicity range shared by ω Cen and NGC 6715, again obtaining a low level of compatibility (15%) with [C/Fe] and [Si/Fe] contributing more to this difference between the two.
– Finally, if these clusters were all ancient NSCs from some galaxy, the basic question would remain of where the clusters associated with ω Cen and its progenitor are. According to simulations (Pfeffer et al. 2018; Pagnini et al. 2023), massive enough progenitors should deposit part of their GCs in the inner Galaxy – that is, in the interval of orbital energies explored in this study – and it is hard to envisage that the clusters that arrived in the Galaxy with ω Cen are among the least chemically compatible with it.

With this work, we have shown that a possible way to proceed in finding clusters that share the same origin (i.e. formed in the same progenitor) is to look for similarities in individual chemical abundances of stars. Individual star abundances keep traces of the different sources (SNe II, AGB stars, SNe Ia, etc.) that may have concurred in producing a stellar system with given chemical characteristics, which are only partially reflected in means, medians, or modes of the distributions in abundance planes (see Appendix G, available on Zenodo). The underlying motivation for looking for similarities in the chemical abundances of different clusters formed in the same progenitor galaxy is that their abundances should, to some extent, reflect those of the ISM in which these clusters were formed; they should share the same genetic heritage. While we do not have direct evidence of how the chemical evolution proceeded in the progenitor galaxy of ω Cen, we do know the chemical abundance patterns of ω Cen itself, which in the hypothesis that ω Cen is the NSC of its host galaxy provide a good representation of the chemical evolution of its host. In Appendix C (available on Zenodo), we indeed show that M54 (NGC 6715), the NSC of the Sagittarius dwarf galaxy, exhibits chemical patterns strikingly similar to those of the Sagittarius galaxy itself. A similar result seems to hold also for the innermost regions of the MW (i.e. the inner degree), whose chemical abundances compare remarkably well with those of the inner disc (Nandakumar et al. 2024).

Once a common chemical link is established between a NSC and its host, it is justified to use the chemical patterns of the NSC – if known – as representative of those of their host galaxy, and hence establish a link with the GC population. This is exactly what we have done in this work, reaching the conclusion that NGC 6656, NGC 6273, NGC 6809, NGC 6205, NGC 6254, and NGC 6752 were all formed in the same progenitor galaxy of which ω Cen is the remnant nucleus. We propose to name this galaxy Nephele – in Greek mythology the mother of Centaurs – to emphasise a common origin for clusters that otherwise would be difficult to associate with each other. Indeed, the most popular way currently used in the literature to associate GCs with their progenitor galaxies, and thus with episodes of accretion onto the MW, is to use their actual kinematic properties. Following such an approach, Massari et al. (2019) classify the above-mentioned GCs as follows: NGC 6205 as one of the clusters associated with the *Gaia* Sausage Enceladus accretion, of which ω Cen would have been the NSC, according to their analysis; NGC 6273, NGC 6809, and NGC 6254 as part of the low-energy group (later identified with Kraken by Kruijssen et al. 2020 or Koala by Forbes 2020); and NGC 6752 and NGC 6656 as disc (i.e. in situ) clusters. Callingham et al. (2022), using a multi-component chemo-dynamical model to split the GC populations, also favour the Kraken origin for NGC 6809, NGC 6273, and NGC 6254, with the addition of NGC 6752, while assigning to NGC 6656 a *Gaia* Sausage Enceladus origin. Making use also of 'kinematic-based' motivations, Myeong et al. (2019) associate ω Cen with the Sequoia galaxy, which should have brought to our Galaxy other GCs, such as FSR 1758, NGC 3201, NGC 6101, NGC 5635, and NGC 6388. Of the above-listed GCs, we could quantify the chemical similarity with ω Cen for three of them: FSR 1758 shows a fraction of stars chemically compatible with ω Cen that is significant, even if affected by large uncertainties (56% ± 26%), while for the other two clusters, NGC 3201 and NGC 6388, our analysis shows no chemical similarity with ω Cen.

In the introduction, we recalled the limitations and lack of physical motivations behind the assumption of 'kinematic coherence' that clusters (and field stars) accreted onto the MW over time should have. Here, we make a step forwards by showing that the kinematic-based classification leads one to establish connections between GCs that do not share common chemical characteristics and to miss connections among GCs that show strong chemical similarities: a possible further reason, other than those already given by Jean-Baptiste et al. (2017); Pagnini et al. (2023), for going beyond this approach.

6. Conclusions

In this paper, we have made use of data from the APOGEE VAC of Galactic GC stars (see Schiavon et al. 2024), which contains full APOGEE DR17 information (Abdurro'uf et al. 2022) for a total of 6422 unique stars associated with 72 Galactic GCs. Following the prediction that ω Cen (NGC 5139) should be the NSC of a galaxy accreted by the MW in the past, our analysis aims to search for the GCs brought by the ω Cen progenitor by looking for common chemical patterns between galactic GCs, and ω Cen, based on individual star abundances. For this purpose, we made use of a GMM approach considering an eight-dimensional abundance space defined by [Fe/H], [Mg/Fe], [Si/Fe], [Ca/Fe], [C/Fe], [Al/Fe], [K/Fe], and [Mn/Fe]. After having fitted the distribution of ω Cen in this eight-dimensional abundance space, we considered the other GCs in the sample and for each of them we estimated the fraction of stars with a high probability of belonging to the GMM model obtained for ω Cen. Apart from ω Cen itself, our analysis allowed us to identify six GCs – namely, NGC 6752, NGC 6656, NGC 6809, NGC 6273, NGC 6205, and NGC 6254 – that have a fraction of stars compatible with ω Cen that is greater than 60%. We suggest that these clusters have potentially been brought into the MW by the progenitor of ω Cen, in this paper referred to as Nephele, the mother of Centaurs. NGC 5024, NGC 6544, FSR 1758, and NGC 1904 – GCs with a fraction greater than 50%, but affected by large uncertainties because of the limited number of available stars – may also be associated with Nephele, although additional work will be needed to understand whether or not they are truly chemically similar with ω Cen. We have divided the clusters that are chemically compatible with ω Cen into two classes – the metal-poor (NGC 6656, NGC 6809, and NGC 6273) one and the metal-rich one (NGC 6752, NGC 6205, and NGC 6254) – as these two groups share other features in addition to the [Fe/H] range. For metal-poor clusters, these are:

– an MDF peak that coincides with the peak of the ω Cen MDF;
– a rising part of the MDF that is comparable to the rising part of the (normalised) MDF of ω Cen;
– no trend of [Mg/Fe] with [Fe/H] (except for NGC 6809, which seems to show a slight decrease in the [Mg/Fe] with increasing [Fe/H]);
– a nearly flat trend in the [Si/Fe] versus [Fe/H] plane;
– a broad distribution in [Mg/Fe], [Si/Fe], [Ca/Fe], [C/Fe], and [K/Fe] with intrinsic dispersions that appear statistically significant in [Mg/Fe], [Ca/Fe], [C/Fe], and [K/Fe], given the reported ASPCAP uncertainties. We note, however, that this result crucially depends on their underestimation (if any).

Metal-rich GCs instead show these peculiarities:

– a decreasing trend of [Mg/Fe] and [Si/Fe] with increasing [Fe/H];
– an extremely [K/Fe]-poor population (except for NGC 6205) that is also present in ω Cen at similar [Fe/H] values;
– their MDFs peak at the same [Fe/H] value, given the uncertainties, and this peak coincides with one of the secondary peaks found in ω Cen MDF (see, for example Johnson & Pilachowski 2010);
– two out of three GCs – namely, NGC 6752 and NGC 6205 – have negatively skewed MDFs;
– their most metal-poor stars have metallicities similar to those at the peak of the ω Cen MDF (at about [Fe/H] $\simeq -1.73$).

Finally, both metal-poor and metal-rich GCs show significant, or non-zero, [Fe/H] intrinsic dispersions, between 0.07 and 0.12 dex. For these dispersions not to be significant, the ASPCAP uncertainties in [Fe/H] should have been underestimated by a factor between 4 and 5, at the metallicities of these clusters. These global characteristics, common to the aforementioned clusters and ω Cen, suggest that these clusters did not evolve chemically independently of each other. Their chemical evolution, on the contrary, must have been closely linked to the environment in which they originated, and thus to the chemical evolution of their galactic progenitor or part of it. In this respect, we would like to comment on the possibility that the evolutionary history of ω Cen is more complex than the one assumed in this paper. For example, Calamida et al. (2020) suggest that ω Cen may be the result of a merger of at least two stellar systems, characterised by different mean metallicities. Our results are not in contradiction with these suggestions, in the sense that, given the current chemical space occupied by ω Cen stars, we derived a sample of clusters that is chemically compatible with it. It is still possible that the two groups of GCs (metal-poor and metal-rich) that we have identified have been formed in different systems, which later merged to form the current ω Cen cluster.

Based on the above-cited similarities, we also tend to rule out the possibility that these GCs are all NSCs of former accreted dwarfs, since this would require that all these NSCs (and their dwarfs) had a very similar chemical evolution, which should be unlikely. As additional support to this conclusion, our analysis shows that M54 (NGC 6715), which is known to be the NSC of the Sagittarius galaxy, is not chemically compatible with ω Cen. Finally, on the basis of their chemical characteristics, we also exclude that ω Cen and its associated clusters formed in galaxies with a chemical enrichment history similar to that experienced, at early times (i.e. similar metallicities), by the Large and Small Magellanic clouds, Sagittarius, and Fornax.

Once placed in kinematic spaces such as the E – L_z space, these GCs turn out to be spread out over an extended region, with some having retrograde orbits and some others direct orbits. For this reason, they have been linked to different galactic progenitors by kinematic-based classifications (see for instance Massari et al. 2019; Myeong et al. 2019; Kruijssen et al. 2020; Forbes 2020; Callingham et al. 2022; Belokurov & Kravtsov 2024). This spread is actually expected since, if Nephele were massive enough compared to the MW (with a mass ratio of about 1/10, as an order of magnitude), simulations show that the energy and angular momentum of its stars and GCs should have not been conserved during its fall into the MW (Jean-Baptiste et al. 2017; Amarante et al. 2022; Pagnini et al. 2023; Khoperskov et al. 2023a,b), and indeed in one of our *N*-body simulations the accreted GCs have a distribution similar to that observed in the E – L_z space for ω Cen and its related GCs. The accretion of other satellite galaxies such as *Gaia* Sausage Enceladus onto the MW has also probably contributed to changing the kinematics of these GCs, and hence their position in the E – L_z space.

Concerning *Gaia* Sausage Enceladus, it is also interesting to mention that while the set of clusters commonly associated (through kinematic methods) with it does not coincide with those that we associate with Nephele, one or two of the Nephele clusters (NGC 6205 and NGC 6656) have been associated in the literature with *Gaia* Sausage Enceladus (Massari et al. 2019; Callingham et al. 2022, as already mentioned). For ω Cen itself, a possible affiliation with *Gaia* Sausage Enceladus has been suggested (Massari et al. 2019). The distribution in E – L_z space of Nephele clusters shows an overlap in kinematic spaces between these two systems. Such an overlap would not be surprising if Nephele and *Gaia* Sausage Enceladus were both massive galaxies relative to the MW, at the time of their accretion. Simulations indeed show that even independent systems, once accreted onto the MW, can be redistributed in similar regions of the kinematic spaces (see e.g. Pfeffer et al. 2018; Pagnini et al. 2023). It is also possible, however, that this overlap hides closer links between Nephele and *Gaia* Sausage Enceladus, which need further analysis.

Overall, our work opens the possibility of connecting different Galactic GCs to the same origin in terms of a progenitor galaxy, suggesting for the first time a different procedure to achieve this goal; namely, that of exploiting the chemical similarities shown by individual chemical abundances. Our results also open new possibilities (and stimulate new questions) of understanding the formation of GCs, whose chemical evolution and related star formation histories appear to be tightly linked to that of the environment in which they formed. A similar conclusion stands also for the Sagittarius dwarf and its NSC NGC 6715 (M54). Consequently, the finding that the formation of star clusters is closely related to the environment in which they formed and that star clusters keep traces of the chemical evolution of their host galaxy seem both to be results of general significance, and not exclusively valid for Nephele and its GCs.

Data availability

Appendices A, B, C, F, and G can be found on Zenodo at the following link: `https://zenodo.org/records/14277327`.

Acknowledgements. The authors are grateful to the referee for their report, which much improved the presentation of the results. The full version of the paper as accepted by the referee can be found on arXiv. The authors wish to thank R. Schiavon for his valuable comments on this work. P.D.M. and M.H. acknowledge the support of the French Agence Nationale de la Recherche (ANR), under grant ANR-13-BS01-0005 (project ANR-20- CE31-0004-01 MWDisc). A.M.B. acknowledges funding from the European Union's Horizon 2020 research and innovation program under the Marie Skłodowska-Curie grant agreement No 895174. F.R. acknowledges support provided by the University of Strasbourg Institute for Advanced Study (USIAS), within the

French national programme Investment for the Future (Excellence Initiative) IdEx-Unistra. O.A. acknowledges support from the Knut and Alice Wallenberg Foundation, the Swedish Research Council (grant 2019-04659), and the Swedish National Space Agency (SNSA Dnr 2023-00164). N.R. acknowledges support from the Swedish Research Council (grant 2023-04744) and the Royal Physiographic Society in Lund through the Stiftelsen Walter Gyllenbergs and Märta och Erik Holmbergs donations. Funding for the Sloan Digital Sky Survey IV has been provided by the Alfred P. Sloan Foundation, the U.S. Department of Energy Office of Science, and the Participating Institutions. SDSS-IV acknowledges support and resources from the Center for High Performance Computing at the University of Utah. The SDSS website is www.sdss.org. SDSS-IV is managed by the Astrophysical Research Consortium for the Participating Institutions of the SDSS Collaboration including the Brazilian Participation Group, the Carnegie Institution for Science, Carnegie Mellon University, Center for Astrophysics Harvard & Smithsonian, the Chilean Participation Group, the French Participation Group, Instituto de Astrofísica de Canarias, The Johns Hopkins University, Kavli Institute for the Physics and Mathematics of the Universe (IPMU)/University of Tokyo, the Korean Participation Group, Lawrence Berkeley National Laboratory, Leibniz Institut für Astrophysik Potsdam (AIP), Max-Planck-Institut für Astronomie (MPIA Heidelberg), Max-Planck-Institut für Astrophysik (MPA Garching), Max-Planck-Institut für Extraterrestrische Physik (MPE), National Astronomical Observatories of China, New Mexico State University, New York University, University of Notre Dame, Observatário Nacional/MCTI, The Ohio State University, Pennsylvania State University, Shanghai Astronomical Observatory, United Kingdom Participation Group, Universidad Nacional Autónoma de México, University of Arizona, University of Colorado Boulder, University of Oxford, University of Portsmouth, University of Utah, University of Virginia, University of Washington, University of Wisconsin, Vanderbilt University, and Yale University. This work has made use of data from the European Space Agency (ESA) mission *Gaia* (https://www.cosmos.esa.int/gaia), processed by the *Gaia* Data Processing and Analysis Consortium (DPAC, https://www.cosmos.esa.int/web/gaia/dpac/consortium). Funding for the DPAC has been provided by national institutions, in particular the institutions participating in the *Gaia* Multilateral Agreement. This work has made use of the computational resources obtained through the DARI grant A0120410154.

References

Abbate, F., Mastrobuono-Battisti, A., Colpi, M., et al. 2018, MNRAS, 473, 927
Abdurro'uf, Accetta, K., Aerts, C., et al. 2022, ApJS, 259, 35
Alfaro-Cuello, M., Kacharov, N., Neumayer, N., et al. 2019, ApJ, 886, 57
Alfaro-Cuello, M., Kacharov, N., Neumayer, N., et al. 2020, ApJ, 892, 20
Alvarez Garay, D. A., Mucciarelli, A., Bellazzini, M., Lardo, C., & Ventura, P. 2024, A&A, 681, A54
Amarante, J. A. S., Debattista, V. P., Beraldo e Silva, L., Laporte, C. F. P., & Deg, N. 2022, ApJ, 937, 12
Antonini, F., Capuzzo-Dolcetta, R., Mastrobuono-Battisti, A., & Merritt, D. 2012, ApJ, 750, 111
Antonini, F., Barausse, E., & Silk, J. 2015, ApJ, 812, 72
Arca-Sedda, M., Capuzzo-Dolcetta, R., Antonini, F., & Seth, A. 2015, ApJ, 806, 220
Bailin, J. 2019, ApJS, 245, 5
Baumgardt, H., & Hilker, M. 2018, MNRAS, 478, 1520
Bekki, K., & Freeman, K. C. 2003, MNRAS, 346, L11
Belokurov, V., & Kravtsov, A. 2024, MNRAS, 528, 3198
Bennett, M., & Bovy, J. 2019, MNRAS, 482, 1417
Bianchini, P., Varri, A. L., Bertin, G., & Zocchi, A. 2013, ApJ, 772, 67
Bovy, J. 2015, ApJS, 216, 29
Calamida, A., Bono, G., Stetson, P. B., et al. 2009, ApJ, 706, 1277
Calamida, A., Zocchi, A., Bono, G., et al. 2020, ApJ, 891, 167
Callingham, T. M., Cautun, M., Deason, A. J., et al. 2022, MNRAS, 513, 4107
Capuzzo-Dolcetta, R. 1993, ApJ, 415, 616
Carraro, G., & Lia, C. 2000, A&A, 357, 977
Carretta, E., Bragaglia, A., Gratton, R., D'Orazi, V., & Lucatello, S. 2009, A&A, 508, 695
Da Costa, G. S. 2016, IAU Symp., 317, 110
Da Costa, G. S., & Marino, A. F. 2011, PASA, 28, 28
Da Costa, G. S., Held, E. V., Saviane, I., & Gullieuszik, M. 2009, ApJ, 705, 1481
D'Orazi, V., Gratton, R. G., Pancino, E., et al. 2011, A&A, 534, A29
Eadie, G. M., Harris, W. E., & Springford, A. 2022, ApJ, 926, 162
Forbes, D. A. 2020, MNRAS, 493, 847
Freeman, K., & Bland-Hawthorn, J. 2002, ARA&A, 40, 487
Gnedin, O. Y., Ostriker, J. P., & Tremaine, S. 2014, ApJ, 785, 71
GRAVITY Collaboration (Abuter, R., et al.) 2019, A&A, 625, L10
Hasselquist, S., Hayes, C. R., Lian, J., et al. 2021, ApJ, 923, 172
Hilker, M., Kayser, A., Richtler, T., & Willemsen, P. 2004, A&A, 422, L9
Horta, D., Schiavon, R. P., Mackereth, J. T., et al. 2023, MNRAS, 520, 5671
Ibata, R. A., Bellazzini, M., Malhan, K., Martin, N., & Bianchini, P. 2019, Nat. Astron., 3, 667
Iben, Icko, J. 1967, ARA&A, 5, 571
Jean-Baptiste, I., Di Matteo, P., Haywood, M., et al. 2017, A&A, 604, A106
Johnson, C. I., & Pilachowski, C. A. 2010, ApJ, 722, 1373
Johnson, C. I., Rich, R. M., Pilachowski, C. A., et al. 2015, AJ, 150, 63
Johnson, C. I., Caldwell, N., Rich, R. M., et al. 2017, ApJ, 836, 168
Kacharov, N., Alfaro-Cuello, M., Neumayer, N., et al. 2022, ApJ, 939, 118
Kamann, S., Husser, T.-O., Dreizler, S., et al. 2018, MNRAS, 473, 5591
Khoperskov, S., Minchev, I., Libeskind, N., et al. 2023a, A&A, 677, A89
Khoperskov, S., Minchev, I., Libeskind, N., et al. 2023b, A&A, 677, A90
Koppelman, H. H., Bos, R. O. Y., & Helmi, A. 2020, A&A, 642, L18
Kruijssen, J. M. D., Pfeffer, J. L., Chevance, M., et al. 2020, MNRAS, 498, 2472
Lacchin, E., Calura, F., & Vesperini, E. 2021, MNRAS, 506, 5951
Lardo, C., Salaris, M., Cassisi, S., et al. 2023, A&A, 669, A19
Lee, Y. W., Joo, J. M., Sohn, Y. J., et al. 1999, Nature, 402, 55
Lehnert, M. D., Bell, R. A., & Cohen, J. G. 1991, ApJ, 367, 514
Leung, H. W., & Bovy, J. 2019a, MNRAS, 483, 3255
Leung, H. W., & Bovy, J. 2019b, MNRAS, 489, 2079
Majewski, S. R., Patterson, R. J., Dinescu, D. I., et al. 2000, Liege Int. Astrophys. Colloq., 35, 619
Marín-Franch, A., Aparicio, A., Piotto, G., et al. 2009, ApJ, 694, 1498
Marino, A. F. 2015, Highlig. Astron., 16, 234
Marino, A. F., Milone, A. P., Piotto, G., et al. 2009, A&A, 505, 1099
Marino, A. F., Milone, A. P., Piotto, G., et al. 2011, ApJ, 731, 64
Massari, D., Koppelman, H. H., & Helmi, A. 2019, A&A, 630, L4
Mastrobuono-Battisti, A., Perets, H. B., & Loeb, A. 2014, ApJ, 796, 40
McKenzie, M., Yong, D., Marino, A. F., et al. 2022, MNRAS, 516, 3515
McMillan, P. J. 2017, MNRAS, 465, 76
Merritt, D., Meylan, G., & Mayor, M. 1997, AJ, 114, 1074
Mészáros, S., Masseron, T., Fernández-Trincado, J. G., et al. 2021, MNRAS, 505, 1645
Meylan, G., & Mayor, M. 1986, A&A, 166, 122
Mucciarelli, A., Lapenna, E., Massari, D., et al. 2015, ApJ, 809, 128
Myeong, G. C., Vasiliev, E., Iorio, G., Evans, N. W., & Belokurov, V. 2019, MNRAS, 488, 1235
Nandakumar, G., Ryde, N., Mace, G., et al. 2024, ApJ, 964, 96
Nitschai, M. S., Neumayer, N., Clontz, C., et al. 2023, ApJ, 958, 8
Norris, J. E., & Da Costa, G. S. 1995, ApJ, 447, 680
Norris, J., & Freeman, K. C. 1983, ApJ, 266, 130
Norris, J. E., Freeman, K. C., & Mighell, K. J. 1996, ApJ, 462, 241
Norris, J. E., Freeman, K. C., Mayor, M., & Seitzer, P. 1997, ApJ, 487, L187
Pagnini, G., Di Matteo, P., Khoperskov, S., et al. 2023, A&A, 673, A86
Pancino, E., Galfo, A., Ferraro, F. R., & Bellazzini, M. 2007, ApJ, 661, L155
Pancino, E., Mucciarelli, A., Sbordone, L., et al. 2011, A&A, 527, A18
Pancino, E., Romano, D., Tang, B., et al. 2017, A&A, 601, A112
Pechetti, R., Kamann, S., Krajnović, D., et al. 2024, MNRAS, 528, 4941
Perets, H. B., & Mastrobuono-Battisti, A. 2014, ApJ, 784, L44
Pfeffer, J., Griffen, B. F., Baumgardt, H., & Hilker, M. 2014, MNRAS, 444, 3670
Pfeffer, J., Kruijssen, J. M. D., Crain, R. A., & Bastian, N. 2018, MNRAS, 475, 4309
Pfeffer, J., Lardo, C., Bastian, N., Saracino, S., & Kamann, S. 2021, MNRAS, 500, 2514
Pilachowski, C., Leep, E. M., Wallerstein, G., & Peterson, R. C. 1982, ApJ, 263, 187
Rain, M. J., Villanova, S., Munõz, C., & Valenzuela-Calderon, C. 2018, MNRAS, 483, 1674
Sanna, N., Pancino, E., Zocchi, A., Ferraro, F. R., & Stetson, P. B. 2020, A&A, 637, A46
Schiavon, R. P., Phillips, S. G., Myers, N., et al. 2024, MNRAS, 528, 1393
Sistero, R. F., & Fourcade, C. R. 1970, AJ, 75, 34
Smith, V. V., Suntzeff, N. B., Cunha, K., et al. 2000, AJ, 119, 1239
Snaith, O. N., Haywood, M., Di Matteo, P., et al. 2014, ApJ, 781, L31
Sollima, A., Pancino, E., Ferraro, F. R., et al. 2005, ApJ, 634, 332
Suntzeff, N. B., & Kraft, R. P. 1996, AJ, 111, 1913
Tremaine, S. D., Ostriker, J. P., & Spitzer, L., J. 1975, ApJ, 196, 407
Tsatsi, A., Mastrobuono-Battisti, A., van de Ven, G., et al. 2017, MNRAS, 464, 3720
Tsuchiya, T., Dinescu, D. I., & Korchagin, V. I. 2003, ApJ, 589, L29
Tsuchiya, T., Korchagin, V. I., & Dinescu, D. I. 2004, MNRAS, 350, 1141
VandenBerg, D. A., Brogaard, K., Leaman, R., & Casagrande, L. 2013, ApJ, 775, 134
Vasiliev, E., & Baumgardt, H. 2021, MNRAS, 505, 5978
Villanova, S., Piotto, G., King, I. R., et al. 2007, ApJ, 663, 296
Villanova, S., Geisler, D., Gratton, R. G., & Cassisi, S. 2014, ApJ, 791, 107
Yong, D., Meléndez, J., Grundahl, F., et al. 2013, MNRAS, 434, 3542

Appendix A: Other clusters chemically compatible with ω Cen: [X/Fe] versus [Fe/H] planes

Available on Zenodo at the following link: https://zenodo.org/records/14277327.

Appendix B: Clusters chemically incompatible with ω Cen but with same metallicity: other examples

Available on Zenodo at the following link: https://zenodo.org/records/14277327.

Appendix C: Are the chemical abundances of a nuclear cluster representative of that of the host galaxy? The case of M54 and the Sagittarius dwarf

Available on Zenodo at the following link: https://zenodo.org/records/14277327.

Appendix D: GCs chemically compatible with ω Cen: other elements

Available on Zenodo at the following link: https://zenodo.org/records/14277327.

Appendix E: On the intrinsic dispersions of abundance ratios for the Galactic GCs chemically compatible with ω Cen

In Sect. 4.2, we have seen that all the Galactic GCs for which we find chemical compatibility with ω Cen show significant intrinsic dispersions, unless the ASPCAP uncertainties on [Fe/H] had been underestimated of a factor between 4 and 5, at the metallicities of these clusters. In Table E.1 we report a similar analysis for all the other abundance ratios that we have used for building the GMM of ω Cen. As in Sect. 4.2, for each cluster, we estimate the total dispersion of the generic [X/Fe] abundance, $\sigma_{\rm [X/Fe],tot}$, the median of [X/Fe] ASPCAP uncertainties for stars in the cluster, $\epsilon_{\rm [X/Fe]}$, and the corresponding $\sigma_{\rm [X/Fe],int}$ defined as $\sqrt{\sigma^2_{\rm [X/Fe],tot} - \epsilon^2_{\rm [X/Fe]}}$.

In general we notice that for all these GCs, the internal dispersions range between 0.04 dex and 0.46 dex, the smallest dispersions being generally found for [Si/Fe], and the largest ones for [Al/Fe]. While the [Si/Fe] dispersions are probably not significant (it is sufficient for ASPCAP uncertainties on this abundance ratio to have been underestimated by 30% to 50%, see parameter A in Table E.1, besides [Al/Fe], which is known to show an extended range of values in Galactic GCs, other abundance ratios seem to be characterised by not null internal dispersions. This is the case of [C/Fe], which shows intrinsic dispersions between 0.2 and 0.3 dex for all these GCs, except for NGC 6254. Note that these dispersions would be not statistically significant if the ASPCAP uncertainties on [C/Fe] had been underestimated of a factor of 3 at least. [Ca/Fe] and [K/Fe] are also elements for which intrinsic dispersions are found for these GCs, unless the corresponding ASPCAP uncertainties had been underestimated by a factor between 2 and 3. Note that such underestimations would lead to a not statistically significant dispersion in [Ca/Fe] and [K/Fe] also for NGC 5139.

Table E.1: Total and intrinsic [X/Fe] dispersions for the metal-poor, the metal-rich GCs chemically compatible with ω Centauri, and ω Cen.

GCname	[X/Fe]	nstars	$\sigma_{\rm [X/Fe],tot}$	$\epsilon_{\rm [X/Fe]}$	$\sigma_{\rm [X/Fe],int}$	A
NGC 6656	[Mg/Fe]	230	0.09	0.03	0.08	2.04
NGC 6656	[Al/Fe]	230	0.40	0.03	0.39	8.55
NGC 6656	[C/Fe]	211	0.32	0.06	0.32	3.75
NGC 6656	[Si/Fe]	230	0.06	0.03	0.05	1.36
NGC 6656	[Ca/Fe]	219	0.17	0.05	0.17	2.54
NGC 6656	[Mn/Fe]	84	0.22	0.05	0.21	3.25
NGC 6656	[K/Fe]	201	0.25	0.09	0.24	2.06
NGC 6809	[Mg/Fe]	58	0.10	0.03	0.09	2.34
NGC 6809	[Al/Fe]	58	0.40	0.03	0.40	10.37
NGC 6809	[C/Fe]	51	0.27	0.05	0.26	3.79
NGC 6809	[Si/Fe]	58	0.05	0.03	0.04	1.27
NGC 6809	[Ca/Fe]	52	0.17	0.04	0.17	2.92
NGC 6809	[Mn/Fe]	24	0.13	0.04	0.12	2.15
NGC 6809	[K/Fe]	57	0.24	0.08	0.23	2.06
NGC 6273	[Mg/Fe]	56	0.12	0.04	0.12	2.38
NGC 6273	[Al/Fe]	56	0.42	0.04	0.41	6.90
NGC 6273	[C/Fe]	56	0.29	0.06	0.28	3.50
NGC 6273	[Si/Fe]	56	0.08	0.04	0.07	1.47
NGC 6273	[Ca/Fe]	54	0.21	0.06	0.20	2.57
NGC 6273	[Mn/Fe]	46	0.15	0.06	0.14	1.97
NGC 6273	[K/Fe]	51	0.29	0.10	0.27	2.08
NGC 6752	[Mg/Fe]	117	0.11	0.03	0.11	3.10
NGC 6752	[Al/Fe]	117	0.44	0.03	0.44	11.31
NGC 6752	[C/Fe]	117	0.22	0.05	0.22	3.08
NGC 6752	[Si/Fe]	117	0.05	0.03	0.04	1.38
NGC 6752	[Ca/Fe]	115	0.13	0.04	0.12	2.29
NGC 6752	[Mn/Fe]	89	0.16	0.04	0.16	2.95
NGC 6752	[K/Fe]	109	0.27	0.08	0.26	2.58
NGC 6205	[Mg/Fe]	34	0.11	0.03	0.11	3.04
NGC 6205	[Al/Fe]	34	0.44	0.03	0.44	10.70
NGC 6205	[C/Fe]	34	0.26	0.05	0.26	3.91
NGC 6205	[Si/Fe]	34	0.06	0.03	0.06	1.62
NGC 6205	[Ca/Fe]	34	0.11	0.04	0.11	2.02
NGC 6205	[Mn/Fe]	26	0.13	0.04	0.12	2.33
NGC 6205	[K/Fe]	34	0.16	0.08	0.14	1.49
NGC 6254	[Mg/Fe]	58	0.12	0.02	0.11	3.29
NGC 6254	[Al/Fe]	58	0.46	0.03	0.46	12.49
NGC 6254	[C/Fe]	58	0.17	0.04	0.16	3.05
NGC 6254	[Si/Fe]	58	0.05	0.02	0.05	1.50
NGC 6254	[Ca/Fe]	57	0.10	0.04	0.09	1.96
NGC 6254	[Mn/Fe]	56	0.13	0.04	0.13	2.47
NGC 6254	[K/Fe]	53	0.23	0.07	0.22	2.28
NGC 5139	[Mg/Fe]	1175	0.19	0.03	0.19	4.59
NGC 5139	[Al/Fe]	1195	0.51	0.03	0.51	11.47
NGC 5139	[C/Fe]	1129	0.32	0.05	0.31	4.32
NGC 5139	[Si/Fe]	1201	0.08	0.03	0.08	1.94
NGC 5139	[Ca/Fe]	1158	0.17	0.04	0.17	2.79
NGC 5139	[Mn/Fe]	721	0.22	0.04	0.21	3.56
NGC 5139	[K/Fe]	1071	0.28	0.08	0.27	2.42

Notes. For each cluster, we also report the median of the [X/Fe] uncertainties of its stars, $\epsilon_{\rm [X/Fe]}$, and the factor A by which these uncertainties would have to be underestimated for the intrinsic dispersions not to be statistically significant.

Appendix F: On the chemical compatibility of ω Cen with the most massive satellites of the Milky Way

Available on Zenodo at the following link: https://zenodo.org/records/14277327.

Appendix G: Median abundances of GCs chemically compatible with ω Cen

Available on Zenodo at the following link: https://zenodo.org/records/14277327.

Appendix H: Testing the reliability of our classification

In this section we test whether the classification shown in Table 1 is robust if [Al/Fe] or [C/Fe] is excluded in the GMM. In fact [Al/Fe] is the element most affected by a possible chemical evolution within the cluster while the value of [C/Fe] depends on the evolutionary phase of the star.

Table H.1 shows, for each cluster, the fraction of stars chemically compatible with ω Cen as in Tab. 1 when considering a seven-dimensional abundance space in the GMM defined by [Fe/H], [Mg/Fe], [Si/Fe],[Ca/Fe], [C/Fe], [K/Fe], and [Mn/Fe]. As we can see, the fractions in this case are in general all much higher than the classification made when also considering [Al/Fe] having 12 clusters (with a total number of stars greater than 15) with compatibility higher than 60% instead of 6. As explained in Sec 3, this should be expected since, by decreasing the dimension of the chemical space, fewer similarity constraints are imposed between clusters so the number of spurious associations increases. Despite this, also in this case all the Nephele's clusters result strongly chemically compatible with ω Cen, having a fraction higher than 70%. Other clusters that share such a high fraction are NGC 6544 (with 15 stars in total), NGC 6218, NGC 288, NGC 6121, and NGC 7089 (with 15 stars in total). We refrain from associating them with Nephele since their similarity is less obvious when considering all the 8 elements in this study (see Tab. 1) but also when retaining [Al/Fe] and removing [C/Fe] (see Tab. H.2).

Table H.2 indeed shows, for each cluster, the same fraction of stars chemically compatible with ω Cen when considering a seven-dimensional abundance space defined by [Fe/H], [Mg/Fe], [Si/Fe],[Ca/Fe], [Al/Fe], [K/Fe], and [Mn/Fe]. In this case, we retrieve that the clusters (with a total number of stars greater than 15) with the highest fraction of stars compatible with ω Cen are the Nephele's GCs, namely: NGC 6656, NGC 6809, NGC 6752, NGC 6254, NGC 6273, NGC 6205. This is the reason why we believe that the association of clusters with Nephele proposed in this study, despite being the result of a more conservative classification, is the most robust. Indeed, finding a similarity between clusters also in [Al/Fe] and [C/Fe] suggests that this group of clusters did not only have to form in an ISM with similar initial composition but also that their IMFs, as well as the dilution they experienced, must have been similar to give rise to such similar final abundance distributions.

Table H.1: Fraction of stars chemically compatible with ω Cen when removing [Al/Fe] in the GMM.

GC name	Fraction (%)	# of stars
Ter10	96 ± 20	1
NGC 5139	**90 ± 3**	**607**
NGC 6656	**90 ± 5**	**68**
NGC 2298	90 ± 25	2
NGC 6752	**88 ± 6**	**83**
NGC 6809	**84 ± 11**	**18**
NGC 6205	**84 ± 11**	**26**
NGC 6522	83 ± 34	2
NGC 6558	81 ± 32	3
Djorg_2	80 ± 31	4
NGC 6544	79 ± 14	15
NGC 6273	**79 ± 8**	**40**
NGC 6218	76 ± 14	40
NGC0288	71 ± 13	37
NGC 6254	**70 ± 14**	**50**
NGC 6121	70 ± 14	169
NGC 7089	70 ± 17	15
NGC 5904	67 ± 15	79
Ter4	65 ± 48	1
NGC 6229	64 ± 37	3
NGC 5024	63 ± 26	5
NGC 6723	62 ± 30	7
NGC 6642	62 ± 26	6
NGC 6171	61 ± 20	23
NGC 1904	60 ± 15	26
NGC 6093	59 ± 49	1
NGC 5272	54 ± 18	71
HP1	52 ± 21	10
NGC 6569	52 ± 28	6
FSR1758	50 ± 26	7
NGC 6380	46 ± 38	9
NGC 6717	45 ± 45	2
NGC 1851	41 ± 20	31
Ter2	40 ± 46	2
Ter9	36 ± 24	9
NGC 3201	36 ± 14	98
NGC 6838	35 ± 21	45
NGC0104	31 ± 24	224
NGC0362	26 ± 19	48
NGC 6715	25 ± 12	26
NGC 2808	24 ± 16	98
NGC 6397	20 ± 20	11
Ter5	15 ± 31	2
NGC 6316	14 ± 25	6
NGC 6760	12 ± 27	3
Pal6	10 ± 30	1
Ton2	4 ± 20	2
NGC 6304	1 ± 4	5
NGC 7078	0 ± 0	1
NGC 6553	0 ± 0	1
NGC 6388	0 ± 0	24
NGC 6293	0 ± 0	1
NGC 4590	0 ± 0	1
NGC 6341	0 ± 0	3

Notes. Nephele's clusters are marked in bold. For each cluster, the number of stars used for the analysis is also shown.

Table H.2: Fraction of stars chemically compatible with ω Cen when removing [C/Fe] in the GMM.

GC name	Fraction (%)	# of stars
Ter10	99 ± 10	1
NGC 5139	**90 ± 3**	**629**
NGC 6656	**89 ± 6**	**71**
NGC 6809	**88 ± 9**	**22**
FSR1758	85 ± 18	7
NGC 6752	**84 ± 6**	**83**
NGC 6254	**82 ± 10**	**50**
NGC 6273	**81 ± 10**	**40**
Ter4	79 ± 41	1
NGC 5024	74 ± 25	5
NGC 6093	73 ± 45	1
NGC 6205	**72 ± 12**	**26**
NGC 2298	62 ± 31	3
NGC 6544	58 ± 18	15
NGC 1904	57 ± 18	28
NGC0288	53 ± 20	37
NGC 6218	48 ± 17	40
NGC 7089	43 ± 22	15
Djorg_2	43 ± 39	4
Ter9	37 ± 24	9
NGC 6121	36 ± 26	169
NGC 6171	31 ± 23	23
NGC 6380	28 ± 28	9
HP1	23 ± 26	10
NGC 6715	22 ± 12	27
NGC 6558	22 ± 31	3
NGC 6397	22 ± 14	15
NGC0104	20 ± 18	224
NGC 6569	20 ± 23	6
NGC 6522	18 ± 33	2
NGC 5272	17 ± 12	72
NGC 6838	16 ± 16	45
NGC 6723	14 ± 20	7
NGC 6642	13 ± 24	6
NGC 6717	13 ± 31	2
NGC 3201	9 ± 10	101
NGC 6229	7 ± 20	3
NGC 5904	6 ± 8	80
Ter2	5 ± 21	2
NGC 6293	5 ± 22	1
NGC 4590	4 ± 20	1
Pal6	2 ± 14	1
Ton2	2 ± 14	2
NGC 6760	1 ± 10	3
NGC 6316	1 ± 8	6
NGC 1851	1 ± 2	31
NGC 6553	0 ± 0	1
NGC 7078	0 ± 0	2
NGC 6388	0 ± 0	24
NGC 6304	0 ± 0	5
NGC 2808	0 ± 0	98
Ter5	0 ± 0	2
NGC0362	0 ± 1	48
NGC 6341	0 ± 0	4

Notes. Nephele's clusters are marked in bold. For each cluster, the number of stars used for the analysis is also shown.